

Systematics of nuclear level density parameters

Till von Egidy¹ and Dorel Bucurescu²

¹Physik-Department, Technische Universität München, D-85748 Garching, Germany

²Horia Hulubei National Institute of Physics and Nuclear Engineering, R-76900 Bucharest, Romania

(Received 1 July 2005; published 27 October 2005)

The level density parameters for backshifted Fermi gas (both without and with energy-dependent level density parameter) and constant-temperature models have been determined for 310 nuclei between ^{18}F and ^{251}Cf by fitting of the complete level schemes at low excitation energies and *s*-wave neutron resonance spacings at the neutron binding energies. Simple formulas are proposed for the description of the two parameters of each of these models, which involve only quantities available from the mass tables. These formulas may constitute a reliable tool for extrapolating to nuclei far from stability, where nuclear level densities cannot be measured.

DOI: [10.1103/PhysRevC.72.044311](https://doi.org/10.1103/PhysRevC.72.044311)

PACS number(s): 21.10.Ma, 21.60.-n

I. INTRODUCTION

Nuclear level densities (LDs) are of special importance in nuclear physics. Indeed, predicting the distribution of all the excited levels of a nucleus presents a great challenge to our understanding of this complicated quantum system. On the other hand, LDs represent a very important ingredient in statistical model calculations of nuclear reaction cross sections, which are needed in many applications from astrophysical calculations (determining thermonuclear rates for nucleosynthesis) to fission or fusion reactor designs.

The direct, experimental determination of LDs is limited both in the number of nuclear species and in the excitation-energy range. Most of the existing experimental data are based on measuring LDs at an energy close to the neutron binding energy, by counting the number of neutron resonances observed in low-energy neutron capture. This kind of measurement is therefore limited to nuclei that are formed by the addition of one neutron to the stable species. In addition, one may determine LDs at lower excitation energies by directly counting the observed excited states, but this procedure is also limited by the accuracy and completeness of the available data. Nevertheless, we often need LDs for many unstable nuclei, for which they cannot be determined experimentally (e.g., in nucleosynthesis calculations). For such nuclei one has to rely on LDs either provided by some theoretical models or extrapolated from nuclei for which experimental information is available. There have been considerable efforts in both these directions (see, e.g. [1,2]), but the extrapolation to nuclei far from the stability line is still rather problematic.

There has been remarkable progress made in theoretical approaches at a microscopic level, such as taking into account shell effects, pairing correlations, and collective effects (see, e.g., the discussion in Refs. [1] and [2]), but their use in practical applications is rather complicated.

On the other hand, most calculations of nuclear LDs are extensions and modifications of the Fermi gas model, to which the pairing and the shell effects are added semiempirically, such as shown for the first time by Gilbert and Cameron [3]. However, the problem of the extrapolation of empirically

determined parameters for such simple models to far-away nuclei persists also in this case, as there is no consistent systematics of these parameters.

For excitation energies not much higher than the neutron separation energy, one can use simple models with only two parameters for the LD, such as the backshifted Fermi gas (BSFG) model [3,4] or the constant-temperature (CT) model [3]. As already emphasized, these simple models do not consider many details of the nuclear interactions; therefore the empirical parameters determined by the fitting of experimental data have complicated variations that implicitly reflect the shell effects, the pairing effects, etc. It is very important for the development of more reliable extrapolation methods to be able to recognize such dependencies and account for them in a simple way.

In this work we follow a heuristic approach to this problem. First, we determine a new set of empirical (phenomenological) LD parameters for such simple models as the BSFG and the CT model by fitting the latest data on low-excitation-energy levels *and* neutron resonance spacings at the neutron binding energies for 310 nuclei. Then we study the variations of these phenomenological parameters for our set of nuclei and observe how they correlate with those of other physical observables. We have considered such observables that are both experimentally known for a large number of nuclei (larger than those in our set) and more reliably calculated theoretically or extrapolated from the existing data. From the observed correlations, we determine simple formulas that describe the main features of our empirical LD data. These formulas are then proposed as reliable means for the extrapolation to unknown nuclei.

The next section of this paper presents the details of the experimental data-fitting procedure and the new phenomenological model parameters. The subsequent section presents the systematics of these parameters and the way we correlate them with different other physical quantities, generally based on the mass tables. The final section presents the adopted formulas that describe the observed systematics and a discussion of their merits. These formulas can be recommended to calculate LDs up to, or slightly higher than, the neutron binding energies. A brief report with these results has recently been presented [5].

II. EMPIRICAL LEVEL DENSITY PARAMETERS

A. The models

For consistency, we subsequently give the formulas of the phenomenological models used in the present study. The LD dependence on the excitation energy U and spin J is assumed to have a separable form:

$$\rho(U, J, \pi) = \frac{1}{2}\rho(U)f(J) \quad (1)$$

where

$$f(J) = e^{J^2/2\sigma^2} - e^{(J+1)^2/2\sigma^2}. \quad (2)$$

We have neglected the dependence of ρ on parity π ; although some parity dependence exists, especially in the case of the low-excitation energies, this dependence is usually ignored.

1. The BSFG model

In the BSFG model [3] we have

$$\rho(U) = \frac{\exp[2\sqrt{a}(U - E_1)]}{12\sqrt{2\sigma}a^{1/4}(U - E_1)^{5/4}}. \quad (3)$$

The function $\exp(2\sqrt{ax})x^{-5/4}$ has a minimum at $x = (25/16)/a$. Therefore ρ was assumed to be constant below $(U - E_1) = (25/16)/a$. This assumption does not influence the final results because it concerns only the first two or three levels in some nuclei; at this low energy the level spacing is large and the weight in the fit is small, as will be explained later. For the spin-cutoff parameter σ we used the following expression proposed in Ref. [6], which is more adequate in the low-energy region:

$$\sigma^2 = 0.0146A^{5/3} \frac{1 + \sqrt{1 + 4a(U - E_1)}}{2a}. \quad (4)$$

The LD parameter a and the excitation-energy shift E_1 (the energy backshift) are considered to be free parameters in our approach and were determined from a fit to the data of each nucleus from our set.

2. The BSFG model with energy dependence of a

Microscopic calculations of LDs show that the shell effects are strongest at low-excitation energies and are damped at high-excitation energies. In the BSFG model the parameter a has been taken to be independent of the energy, which means assuming that the shell effects continue to play a role at higher energies in the same way as at low energies. To include the damping of the shell effects, the following expression was proposed phenomenologically for the LD parameter [7,8] that is inspired from microscopic treatments of the LD that show that a must have an energy dependence:

$$a(U, Z, N) = \tilde{a} \left[1 + \frac{S(Z, N) - \Delta}{U - E_2} f(U - E_2) \right], \quad (5)$$

where \tilde{a} is the asymptotic value of the a parameter (at high-excitation energies). For the function f the following form has been proposed [7,9,10]:

$$f(U - E_2) = 1 - e^{-\gamma(U - E_2)}, \quad (6)$$

$S(Z, N)$ is the so-called shell correction (or shell correction in the mass formula) defined as

$$S(Z, N) = M_{\text{exp}} - M_{\text{LD}}, \quad (7)$$

where M_{exp} is the experimental mass and M_{LD} is the mass calculated with a macroscopic liquid-drop formula. The formula that we use for the liquid-drop mass is defined in Eq. (9) in Sec. III. It does not include a pairing term. Therefore the pairing Δ has to be subtracted, and this is discussed later. Here we emphasize that in our present approach we use a formula for a spherical drop; this differs from other approaches that use liquid-drop energies calculated for equilibrium shapes of nuclei [7,8,10]. We judge this choice from the point of view of the results we get and of a certain advantage for extrapolations to nuclei far from stability. In formula (5) we use $\gamma = 0.06 \text{ MeV}^{-1}$, close to the values obtained, e.g., in Refs. [7,8,10]. In this approach the two free parameters that we determine from the fit to the data of each nucleus are \tilde{a} and the corresponding backshift energy E_2 .

3. The CT model

The third model used is the CT model [3], with

$$\rho(U) = \frac{1}{T} e^{(U - E_0)/T}. \quad (8)$$

For the spin-cutoff parameter σ , the formula $\sigma = 0.98A^{0.29}$ of Ref. [11] has been used in this case, because it is the most simple experimental formula and Eq. (4) cannot be used because it depends on a . The two free parameters of the model are the temperature T and the backshift energy E_0 . It was noted earlier that this simple model can also give good fits to data at both low energies and the neutron binding energy [11].

B. The fit procedure and results

The set of data to which we fit the preceding LD formulas contains 310 nuclei between ^{19}F and ^{251}Cf . For these nuclei we have taken into consideration the current information on both the low-energy excited states [12] in a certain spin window and up to a certain excitation energy and on the LD at the neutron resonance energy [13]. The completeness of the low-energy level scheme plays an important role. We checked it very carefully in the given energy and spin range. To judge the completeness we used our own experience, because we have been involved in level scheme construction for several decades. The level schemes are established by a large number of reactions and compared with theoretical expectations. The agreement between the predicted and measured level structure is frequently a good argument for the completeness. We assume that about 95% of the used levels are correctly placed. Table I lists all experimental quantities considered in the empirical fits. Additionally, the fifth, sixth, and seventh columns show the deuteron pairing, the shell correction, and its derivative, respectively all used for the interpretation of the LD parameters.

Each of the models considered has two free parameters, which were fitted to the aforementioned data according to the procedure outlined in Ref. [11]: Namely, the calculated level

TABLE I. Experimental data used for the determination of LD parameters. The second, third, and fourth columns give information concerning the low-energy discrete levels; the last three columns give information concerning the LD at neutron binding energies; and the fifth, sixth, and seventh columns contain the deuteron pairing, the shell correction [calculated with Eqs. (7) and (9)], and its derivative with respect to the mass [Eq. (12)].

Nucleus	Energy range (MeV)	Spin window (\hbar)	Number of levels	Deuteron pairing ^a (MeV)	Shell energy ^b (MeV)	Δ Shell energy ^c (MeV)	n binding energy (MeV)	Spin (\hbar)	Density (per MeV)
¹⁸ F	6.88	0–4	47	-6.763	1.586	0.900	9.149		
¹⁹ F	8.32	1/2–11/2	60	-1.783	1.792	0.383	10.432		
²⁰ F	4.60	0–3	26	-4.386	4.131	0.005	6.601	0–1	6(2)
²⁰ Ne	13.97	0–6	103	-4.886	-3.358	-0.028	16.865		
²³ Na	8.98	1/2–7/2	77	0.068	0.174	-0.278	12.419		
²⁴ Na	4.57	0–4	30	-3.702	2.854	-0.307	6.960	1–2	11(3)
²⁴ Mg	12.00	0–4	66	-5.237	-4.325	-0.292	16.531		
²⁵ Mg	7.97	1/2–9/2	58	0.170	-0.339	-0.357	7.331	1/2	2(1)
²⁶ Mg	8.58	0–4	51	-3.580	-1.503	-0.412	11.093	2–3	23(9)
²⁷ Mg	5.93	1/2–7/2	31	-0.800	0.726	-0.348	6.443	1/2	4(1)
²⁶ Al	8.19	0–5	160	-5.503	0.305	-0.451	11.366		
²⁷ Al	8.00	1/2–11/2	65	-0.347	-1.256	-0.651	13.058		
²⁸ Al	5.01	1–4	33	-3.473	1.206	-0.407	7.725	2–3	22(7)
²⁸ Si	11.59	0–6	62	-5.287	-6.129	-0.591	17.180		
²⁹ Si	9.00	1/2–9/2	68	-1.076	-2.943	-0.327	8.474	1/2	5(2)
³⁰ Si	9.97	0–4	77	-3.855	-3.133	-0.269	10.609	0–1	3(1)
³⁰ P	8.02	0–5	107	-3.554	-2.060	0.237	11.319		
³¹ P	7.15	1/2–9/2	45	0.200	-2.564	0.266	12.312		
³² P	4.88	0–4	35	-2.877	0.132	0.166	7.936	0–1	13(4)
³² S	8.87	0–4	44	-3.696	-5.181	0.265	15.042		
³³ S	4.95	1/2–11/2	22	0.141	-1.877	0.247	8.642	1/2	7(2)
³⁴ S	6.49	0–4	25	-3.018	-2.470	0.179	11.417	1–2	37(14)
³⁵ S	4.11	1/2–7/2	17	0.203	0.332	0.242	6.986	1/2	5(2)
³⁶ Cl	3.97	1–3	19	-2.801	0.848	0.228	8.580	1–2	44(11)
³⁸ Cl	1.99	0–3	8	-3.054	3.523	0.560	6.108	1–2	67(18)
³⁸ Ar	8.00	0–6	80	-3.186	-1.557	0.360	11.838		
⁴⁰ Ar	5.98	0–6	58	-2.630	1.510	0.270	9.869		
⁴¹ Ar	2.41	1/2–5/2	9	0.129	3.901	0.006	6.099	1/2	14(4)
⁴⁰ K	3.49	1–3	28	-3.096	2.287	0.343	7.800	1–2	67(22)
⁴¹ K	5.03	5/2–9/2	50	-0.266	2.594	0.100	10.095	7/2–9/2	400(43)
⁴² K	1.26	0–6	12	-3.233	4.603	-0.109	7.534	1–2	67(22)
⁴⁰ Ca	8.49	0–4	57	-4.385	-4.209	0.288	15.643		
⁴¹ Ca	4.10	1/2–11/2	26	-0.140	-0.168	0.573	8.363	1/2	31(4)
⁴³ Ca	2.28	1/2–7/2	13	-0.095	2.459	-0.055	7.933	1/2	50(13)
⁴⁴ Ca	3.72	0–4	13	-3.079	1.076	-0.262	11.131	3–4	556(93)
⁴⁵ Ca	2.85	1/2–7/2	15	-0.349	2.628	-0.402	7.415	1/2	41(6)
⁴⁶ Sc	1.93	2–5	27	-3.221	3.554	-0.409	8.761	3–4	769(59)
⁴⁷ Ti	2.53	1/2–5/2	12	-0.420	0.945	-0.540	8.880	1/2	40(7)
⁴⁸ Ti	4.08	0–4	20	-2.998	-0.562	-0.597	11.627	2–3	570(80)
⁴⁹ Ti	2.67	1/2–7/2	11	-0.292	0.680	-0.600	8.142	1/2	55(9)
⁵⁰ Ti	4.95	0–4	14	-3.458	-1.570	-0.261	10.939	3–4	250(50)
⁵¹ Ti	3.24	1/2–7/2	12	-0.527	0.088	0.266	6.372	1/2	8(4)
⁵¹ V	3.39	1/2–9/2	17	0.280	-0.309	-0.395	11.051	1/2	430(110)
⁵² V	2.11	1–5	15	-2.738	1.277	0.011	7.311	3–4	240(40)
⁵¹ Cr	3.01	1/2–9/2	20	-0.126	-1.124	-0.642	9.261	1/2	75(7)
⁵³ Cr	3.00	1/2–7/2	14	-0.329	-0.902	-0.172	7.939	1/2	23(2)
⁵⁴ Cr	3.93	0–4	16	-2.757	-1.527	-0.066	9.719	1–2	130(13)
⁵⁵ Cr	2.60	1/2–9/2	16	-0.440	0.694	-0.005	6.246	1/2	16(2)
⁵⁶ Mn	2.11	1–3	31	-2.633	1.013	-0.089	7.270	2–3	430(80)
⁵⁵ Fe	2.58	1/2–7/2	11	-0.463	-3.274	-0.265	9.298	1/2	56(7)
⁵⁷ Fe	3.00	1/2–9/2	36	-0.211	-1.293	-0.083	7.646	1/2	39(4)
⁵⁸ Fe	3.76	0–4	17	-2.874	-1.882	-0.052	10.045	0–1	154(24)

TABLE I. (*Continued.*)

Nucleus	Energy range (MeV)	Spin window (\hbar)	Number of levels	Deuteron pairing ^a (MeV)	Shell energy ^b (MeV)	Δ Shell energy ^c (MeV)	n binding energy (MeV)	Spin (\hbar)	Density (per MeV)
⁵⁹ Fe	2.17	1/2–7/2	15	-0.471	0.395	-0.128	6.581	1/2	39(8)
⁶⁰ Co	2.32	2–5	37	-2.801	0.805	-0.098	7.492	3–4	800(96)
⁵⁹ Ni	2.49	1/2–7/2	13	-0.492	-3.637	0.097	8.999	1/2	75(5)
⁶⁰ Ni	3.60	0–3	12	-3.150	-4.020	0.082	11.388	1–2	500(180)
⁶¹ Ni	2.70	1/2–9/2	25	-0.317	-1.460	0.053	7.820	1/2	73(5)
⁶² Ni	3.47	0–4	14	-3.209	-2.274	0.025	10.597	1–2	480(34)
⁶³ Ni	1.46	1/2–7/2	9	-0.432	0.098	-0.039	6.838	1/2	63(12)
⁶⁵ Ni	1.93	1/2–7/2	11	-0.546	1.143	-0.133	6.098	1/2	51(8)
⁶⁴ Cu	1.51	0–3	22	-2.399	0.903	0.349	7.916	1–2	1050(100)
⁶⁶ Cu	1.98	0–3	28	-2.295	2.138	0.326	7.066	1–2	770(70)
⁶⁵ Zn	1.95	1/2–5/2	14	0.318	0.103	0.412	7.979	1/2	280(13)
⁶⁷ Zn	1.69	1/2–7/2	18	0.415	1.601	0.368	7.052	1/2	216(26)
⁶⁸ Zn	3.41	0–4	16	-2.423	0.407	0.303	10.198	2–3	2500(380)
⁶⁹ Zn	2.09	1/2–5/2	18	0.312	2.425	0.347	6.482	1/2	180(14)
⁷¹ Zn	1.80	1/2–5/2	10	0.391	2.936	0.247	5.834	1/2	140(15)
⁷⁰ Ga	1.27	0–4	16	-2.386	3.349	0.235	7.654	0–1	2860(490)
⁷² Ga	1.04	0–4	20	-2.904	4.389	0.085	6.520	1–2	2630(420)
⁷¹ Ge	1.61	1/2–7/2	29	0.234	2.778	0.312	7.416	1/2	1120(300)
⁷³ Ge	1.16	1/2–9/2	21	0.289	3.395	0.151	6.783	1/2	667(130)
⁷⁴ Ge	2.98	0–4	24	-2.983	1.562	0.032	10.196	4–5	16 100(3900)
⁷⁵ Ge	1.43	1/2–9/2	24	-0.048	2.967	-0.010	6.505	1/2	330(110)
⁷⁷ Ge	1.05	1/2–9/2	14	-0.163	1.999	-0.064	6.072	1/2	220(70)
⁷⁶ As	0.81	0–4	37	-2.935	4.518	-0.034	7.328	1–2	13 000(1350)
⁷⁵ Se	1.21	1/2–7/2	26	-0.073	3.070	-0.011	8.028	1/2	2940(690)
⁷⁷ Se	1.01	1/2–7/2	16	-0.049	3.240	-0.058	7.419	1/2	1540(240)
⁷⁸ Se	2.91	0–6	28	-2.937	1.425	-0.122	10.498	0–1	9100(2500)
⁷⁹ Se	1.50	1/2–9/2	28	0.028	2.709	-0.156	6.963	1/2	500(125)
⁸¹ Se	1.84	1/2–9/2	19	-0.067	1.334	-0.314	6.701	1/2	500(200)
⁸³ Se	1.72	1/2–5/2	15	0.231	-0.099	-0.310	5.818	1/2	200(100)
⁸⁰ Br	0.78	0–5	36	-2.918	4.029	-0.201	7.892	1–2	21 300(2300)
⁸² Br	1.00	0–5	22	-2.599	2.672	-0.319	7.593	1–2	9500(1400)
⁷⁹ Kr	1.14	1/2–11/2	30	-0.098	2.712	-0.155	8.334	1/2	4000(1300)
⁸¹ Kr	1.40	1/2–7/2	21	-0.122	2.608	-0.220	7.873	1/2	3570(770)
⁸⁴ Kr	3.23	0–5	16	-2.309	-0.659	-0.557	10.521	4–5	5000(2500)
⁸⁵ Kr	2.75	1/2–9/2	30	0.323	-0.030	-0.561	7.121	1/2	1000(100)
⁸⁶ Rb	1.83	0–5	24	-2.429	0.445	-0.707	8.651	2–3	5900(1000)
⁸⁸ Rb	1.92	0–4	21	-1.995	-0.123	0.154	6.082	1–2	560(90)
⁸⁵ Sr	1.99	1/2–9/2	27	-0.056	0.996	-0.619	8.530	1/2	3100(1200)
⁸⁷ Sr	3.24	1/2–3/2	17	0.054	-0.823	-0.880	8.428	1/2	385(118)
⁸⁸ Sr	4.31	0–5	17	-3.305	-3.489	-0.359	11.113	4–5	3400(1000)
⁸⁹ Sr	3.14	1/2–9/2	18	-0.738	-1.787	0.214	6.359	1/2	42(5)
⁹⁰ Y	2.19	0–3	16	-1.700	-0.992	0.354	6.857	0–1	270(30)
⁹¹ Zr	2.94	1/2–9/2	25	-0.435	-2.163	0.456	7.195	1/2	167(39)
⁹² Zr	3.20	0–5	19	-2.028	-2.071	0.431	8.635	2–3	1820(330)
⁹³ Zr	2.19	1/2–5/2	12	-0.554	-0.454	0.362	6.734	1/2	286(65)
⁹⁴ Zr	2.37	0–4	9	-2.058	-0.689	0.346	8.221	2–3	6250(590)
⁹⁵ Zr	2.38	1/2–5/2	11	-0.743	0.482	0.273	6.462	1/2	310(80)
⁹⁷ Zr	2.27	1/2–9/2	10	-1.180	1.293	0.494	5.575	1/2	77(18)
⁹⁴ Nb	1.01	2–5	23	-2.258	0.733	0.231	7.228	4–5	12 500(1600)
⁹³ Mo	2.55	1/2–9/2	19	-0.479	-3.057	0.201	8.070	1/2	370(70)
⁹⁵ Mo	1.43	1/2–7/2	11	-0.493	-0.984	0.163	7.369	1/2	758(103)
⁹⁶ Mo	2.60	0–4	17	-2.394	-1.149	0.214	9.154	2–3	9520(910)
⁹⁷ Mo	1.57	1/2–7/2	25	-0.488	0.653	0.160	6.821	1/2	950(180)
⁹⁸ Mo	2.58	0–6	28	-2.302	0.279	0.261	8.643	2–3	13 300(3600)
⁹⁹ Mo	1.26	1/2–9/2	23	0.005	2.276	0.252	5.925	1/2	1000(200)

TABLE I. (*Continued.*)

Nucleus	Energy range (MeV)	Spin window (\hbar)	Number of levels	Deuteron pairing ^a (MeV)	Shell energy ^b (MeV)	Δ Shell energy ^c (MeV)	n binding energy (MeV)	Spin (\hbar)	Density (per MeV)
¹⁰¹ Mo	0.99	1/2–9/2	34	-0.049	3.433	0.013	5.398	1/2	1250(230)
¹⁰⁰ Tc	0.72	2–5	27	-2.589	3.014	0.029	6.764	4–5	83 300(9000)
¹⁰⁰ Ru	2.50	0–6	23	-2.618	-0.994	-0.024	9.673	2–3	40 000(6400)
¹⁰² Ru	2.05	0–4	13	-2.615	0.397	-0.044	9.220	2–3	55 600(9300)
¹⁰³ Ru	0.88	1/2–11/2	27	-0.168	2.360	-0.122	6.232	1/2	1820(500)
¹⁰⁵ Ru	0.89	1/2–5/2	23	-0.197	2.962	-0.173	5.910	1/2	3330(830)
¹⁰⁴ Rh	0.74	1–3	40	-2.550	2.837	-0.098	6.999	0–1	31 300(3900)
¹⁰⁵ Pd	1.11	1/2–9/2	23	-0.201	0.785	-0.137	7.094	1/2	4170(520)
¹⁰⁶ Pd	2.41	0–4	21	-2.627	0.006	-0.144	9.561	2–3	97 100(4700)
¹⁰⁷ Pd	0.79	1/2–11/2	15	-0.083	1.922	-0.138	6.536	1/2	3700(1200)
¹⁰⁸ Pd	2.43	0–6	20	-2.613	0.826	-0.129	9.228	2–3	90 900(7400)
¹⁰⁹ Pd	0.68	1/2–7/2	20	-0.065	2.490	-0.128	6.154	1/2	5490(1000)
¹¹¹ Pd	0.67	1/2–9/2	16	0.018	2.678	-0.157	5.726	1/2	6700(2200)
¹⁰⁸ Ag	0.69	0–4	26	-2.526	2.260	-0.178	7.271	0–1	45 500(8300)
¹¹⁰ Ag	0.71	1–3	45	-2.592	3.093	-0.206	6.809	0–1	66 200(6100)
¹⁰⁷ Cd	1.60	1/2–7/2	26	-0.206	-1.177	-0.169	7.924	1/2	7410(1920)
¹⁰⁹ Cd	1.48	1/2–7/2	23	-0.110	0.193	-0.204	7.327	1/2	8300(2100)
¹¹¹ Cd	1.56	1/2–7/2	36	-0.211	1.016	-0.251	6.976	1/2	6450(830)
¹¹² Cd	2.16	0–4	13	-2.564	0.003	-0.306	9.394	0–1	50 000(10 000)
¹¹³ Cd	1.41	1/2–7/2	42	-0.171	1.538	-0.294	6.540	1/2	5260(690)
¹¹⁴ Cd	2.81	0–3	30	-2.584	0.271	-0.308	9.043	0–1	40 300(4200)
¹¹⁵ Cd	1.37	1/2–7/2	27	-0.102	1.614	-0.314	6.141	1/2	4260(630)
¹¹⁷ Cd	1.36	1/2–7/2	19	-0.080	1.256	-0.380	5.777	1/2	2560(590)
¹¹⁴ In	0.84	2–5	12	-2.482	1.870	-0.350	7.274	4–5	76 900(17 700)
¹¹⁶ In	0.90	3–4	20	-2.588	2.150	-0.399	6.785	4–5	105 300(5500)
¹¹³ Sn	1.87	1/2–7/2	24	-0.633	-0.775	-0.018	7.743	1/2	6370(2110)
¹¹⁵ Sn	1.86	1/2–7/2	11	-1.029	-0.453	-0.074	7.546	1/2	3500(1300)
¹¹⁶ Sn	3.98	0–4	65	-3.242	-1.397	-0.054	9.563	0–1	21 700(6600)
¹¹⁷ Sn	2.09	1/2–7/2	25	-0.893	-0.022	-0.123	6.943	1/2	2630(900)
¹¹⁸ Sn	2.50	0–4	13	-3.319	-1.324	-0.121	9.327	0–1	18 200(1700)
¹¹⁹ Sn	1.99	1/2–7/2	29	-0.798	-0.068	-0.178	6.484	1/2	2080(390)
¹²⁰ Sn	2.47	0–4	13	-3.325	-1.717	-0.227	9.108	0–1	11 100(2500)
¹²¹ Sn	1.50	1/2–7/2	18	-0.740	-0.702	-0.267	6.170	1/2	610(74)
¹²³ Sn	1.50	1/2–7/2	16	-0.772	-1.885	-0.358	5.946	1/2	600(180)
¹²⁵ Sn	1.90	1/2–7/2	15	-0.835	-3.551	-0.436	5.733	1/2	200(48)
¹²² Sb	0.65	1–4	19	-2.485	1.065	0.104	6.806	2–3	76 900(11 800)
¹²⁴ Sb	0.76	2–5	25	-2.385	-0.006	0.057	6.467	3–4	41 700(5200)
¹²³ Te	1.89	1/2–7/2	45	0.044	0.416	0.000	6.929	1/2	7580(860)
¹²⁴ Te	3.00	0–4	44	-2.404	-1.301	-0.024	9.424	0–1	58 800(10 400)
¹²⁵ Te	2.19	1/2–7/2	71	0.081	-0.432	-0.008	6.569	1/2	5260(550)
¹²⁶ Te	2.85	0–6	46	-2.385	-2.370	-0.034	9.114	0–1	26 300(3500)
¹²⁷ Te	2.20	1/2–7/2	71	0.098	-1.739	-0.003	6.288	1/2	1820(330)
¹²⁹ Te	2.20	1/2–7/2	50	0.069	-3.516	0.003	6.082	1/2	1350(270)
¹³¹ Te	2.40	1/2–7/2	36	0.048	-5.739	0.008	5.929	1/2	670(220)
¹²⁸ I	0.43	1–5	23	-2.235	-0.144	-0.050	6.826	2–3	66 700(13 300)
¹³⁰ I	0.39	2–5	21	-2.204	-1.641	-0.042	6.500	3–4	33 300(3300)
¹²⁹ Xe	1.00	1/2–9/2	20	-0.176	-0.733	-0.013	6.909	1/2	4000(1600)
¹³⁰ Xe	2.39	0–6	23	-2.435	-2.568	-0.039	9.256	0–1	26 300(3500)
¹³¹ Xe	1.04	1/2–7/2	14	-0.128	-2.005	-0.015	6.605	1/2	4350(1130)
¹³² Xe	3.08	2–5	30	-2.369	-4.021	-0.051	8.937	1–2	20 400(6300)
¹³³ Xe	1.36	1/2–7/2	13	-0.130	-3.778	-0.033	6.434	1/2	1330(420)
¹³⁵ Xe	2.49	1/2–9/2	27	-0.201	-6.046	-0.036	6.364	1/2	625(230)
¹³⁷ Xe	2.29	1/2–9/2	42	-0.134	-6.414	1.032	4.026	1/2	77(36)
¹³⁴ Cs	0.63	2–5	26	-2.193	-1.847	-0.054	6.892	3–4	47 600(4500)
¹³⁵ Cs	1.07	5/2–7/2	6	-0.101	-3.807	-0.110	8.762	7/2–9/2	62 500(11 700)

TABLE I. (*Continued.*)

Nucleus	Energy range (MeV)	Spin window (\hbar)	Number of levels	Deuteron pairing ^a (MeV)	Shell energy ^b (MeV)	Δ Shell energy ^c (MeV)	n binding energy (MeV)	Spin (\hbar)	Density (per MeV)
^{131}Ba	1.32	1/2–5/2	19	-0.186	0.023	-0.026	7.494	1/2	17 240(3000)
^{133}Ba	1.36	1/2–5/2	19	-0.198	-0.912	-0.064	7.190	1/2	9090(2900)
^{135}Ba	1.01	1/2–5/2	8	-0.265	-2.292	-0.059	6.972	1/2	2700(260)
^{136}Ba	2.44	0–5	18	-2.179	-4.237	-0.150	9.108	1–2	25 000(3800)
^{137}Ba	2.41	1/2–7/2	18	-0.315	-4.220	-0.094	6.906	1/2	826(81)
^{138}Ba	3.25	0–4	18	-2.932	-6.142	0.383	8.612	1–2	3850(740)
^{139}Ba	2.58	1/2–5/2	20	-0.172	-4.406	0.842	4.723	1/2	53(8)
^{139}La	1.77	1/2–9/2	15	0.651	-4.184	0.299	8.778	9/2–11/2	31 250(5860)
^{140}La	0.80	1–5	20	-2.079	-2.536	0.719	5.161	3–4	4500(800)
^{137}Ce	1.48	1/2–7/2	17	-0.142	-1.243	-0.129	7.482	1/2	20 000(8000)
^{141}Ce	2.21	1/2–9/2	20	-0.288	-3.026	0.679	5.428	1/2	320(50)
^{142}Ce	2.81	0–3	24	-2.000	-3.268	0.589	7.170	3–4	15 400(4700)
^{143}Ce	1.23	1/2–9/2	16	-0.327	-1.712	0.583	5.145	1/2	910(410)
^{142}Pr	0.75	1–4	12	-2.125	-1.389	0.578	5.843	2–3	9100(1600)
^{143}Nd	2.41	1/2–5/2	22	-0.360	-2.243	0.542	6.124	1/2	1160(110)
^{144}Nd	2.70	0–5	29	-2.127	-2.445	0.493	7.817	3–4	28 600(4100)
^{145}Nd	2.06	1/2–7/2	35	-0.376	-0.816	0.471	5.755	1/2	2220(250)
^{146}Nd	2.29	0–4	30	-2.117	-1.225	0.492	7.565	3–4	58 800(10 400)
^{147}Nd	1.05	1/2–5/2	15	-0.300	0.416	0.468	5.292	1/2	3450(590)
^{148}Nd	1.87	0–3	14	-2.255	-0.203	0.413	7.333	2–3	286 000(139 000)
^{149}Nd	0.99	1/2–7/2	31	0.044	1.257	0.208	5.039	1/2	6450(830)
^{151}Nd	0.74	1/2–7/2	20	-0.082	0.912	-0.095	5.335	1/2	6060(550)
^{148}Pm	0.40	1–2	12	-2.122	1.788	0.402	5.895	3–4	192 000(44 000)
^{145}Sm	2.20	1/2–11/2	26	-0.400	-2.024	0.441	6.757	1/2	1490(130)
^{148}Sm	2.40	0–5	36	-2.214	-0.734	0.407	8.141	3–4	196 000(19 000)
^{149}Sm	1.06	1/2–11/2	27	-0.288	0.995	0.391	5.871	1/2	10 000(2000)
^{150}Sm	2.05	0–6	37	-2.174	0.384	0.342	7.987	3–4	476 000(68 000)
^{151}Sm	0.96	1/2–3/2	22	0.140	1.943	0.077	5.596	1/2	21 700(3800)
^{152}Sm	1.59	0–6	19	-2.095	0.625	-0.078	8.258	3–4	962 000(139 000)
^{153}Sm	0.49	1/2–9/2	21	0.044	1.484	-0.094	5.868	1/2	20 800(2200)
^{155}Sm	0.99	1/2–5/2	19	-0.121	0.543	-0.068	5.807	1/2	8770(1150)
^{152}Eu	0.35	1–4	63	-2.491	3.157	0.099	6.307	2–3	1 370 000(131 000)
^{153}Eu	0.74	1/2–9/2	22	0.044	1.870	-0.057	8.550	5/2–7/2	1 790 000(320 000)
^{154}Eu	0.49	1–5	74	-1.911	2.477	-0.073	6.442	2–3	910 000(165 000)
^{155}Eu	1.11	1/2–7/2	25	0.126	1.164	-0.141	8.151	5/2–7/2	1 087 000(142 000)
^{156}Eu	0.39	0–5	27	-1.486	1.455	-0.078	6.340	2–3	232 600(81 100)
^{153}Gd	0.80	1/2–9/2	49	0.067	2.087	-0.022	6.247	1/2	71 400(15 000)
^{155}Gd	1.09	1/2–5/2	32	-0.005	1.713	-0.118	6.435	1/2	69 400(7200)
^{156}Gd	1.97	0–4	35	-1.931	0.333	-0.149	8.536	1–2	588 000(69 000)
^{157}Gd	0.93	1/2–7/2	26	-0.149	0.920	-0.091	6.360	1/2	33 300(6700)
^{158}Gd	2.08	0–4	45	-1.729	-0.276	-0.045	7.937	1–2	204 000(21 000)
^{159}Gd	1.30	1/2–5/2	34	-0.101	0.319	-0.053	5.943	1/2	12 200(900)
^{161}Gd	0.91	1/2–11/2	21	-0.185	-0.282	-0.078	5.635	1/2	5000(500)
^{160}Tb	0.39	0–5	27	-1.599	1.274	-0.068	6.375	1–2	238 000(17 000)
^{157}Dy	0.53	1/2–7/2	20	-0.133	1.725	-0.058	6.969	1/2	208 000(70 000)
^{159}Dy	0.59	1/2–9/2	16	-0.187	1.202	-0.045	6.833	1/2	45 500(23 000)
^{161}Dy	0.87	1/2–5/2	20	-0.100	0.695	-0.045	6.454	1/2	37 000(6900)
^{162}Dy	1.90	0–5	37	-1.772	-0.547	-0.068	8.197	2–3	417 000(35 000)
^{163}Dy	0.96	1/2–7/2	26	-0.200	-0.062	-0.088	6.271	1/2	16 100(1300)
^{164}Dy	2.01	0–5	35	-1.594	-1.161	-0.024	7.658	2–3	147 000(13 000)
^{165}Dy	0.74	1/2–9/2	22	-0.174	-0.512	-0.042	5.716	1/2	6700(500)
^{166}Ho	0.64	0–7	43	-1.408	0.297	-0.018	6.244	3–4	238 000(28 000)
^{163}Er	0.71	1/2–7/2	21	-0.105	1.121	-0.036	6.903	1/2	125 000(31 000)
^{165}Er	1.01	1/2–9/2	41	-0.062	0.553	-0.044	6.650	1/2	47 600(9100)
^{167}Er	0.90	1/2–11/2	30	-0.204	-0.233	0.005	6.436	1/2	26 300(2100)

TABLE I. (*Continued.*)

Nucleus	Energy range (MeV)	Spin window (\hbar)	Number of levels	Deuteron pairing ^a (MeV)	Shell energy ^b (MeV)	Δ Shell energy ^c (MeV)	n binding energy (MeV)	Spin (\hbar)	Density (per MeV)
^{168}Er	2.10	0–6	65	-1.558	-1.234	-0.030	7.771	3–4	238 000(17 000)
^{169}Er	0.86	1/2–11/2	23	-0.178	-0.659	-0.029	6.003	1/2	10 000(1000)
^{171}Er	0.71	1/2–9/2	13	-0.194	-1.001	-0.054	5.682	1/2	6800(930)
^{170}Tm	0.48	0–6	26	-1.328	0.177	-0.001	6.592	0–1	118 000(10 000)
^{171}Tm	1.29	1/2–7/2	16	-0.027	-0.626	-0.040	7.486	1/2–3/2	256 000(66 000)
^{169}Yb	0.84	1/2–11/2	26	-0.179	0.367	0.010	6.867	1/2	125 000(47 000)
^{170}Yb	2.44	0–2	30	-1.739	-0.742	0.025	8.470	3–4	625 000(16 000)
^{171}Yb	1.03	1/2–13/2	30	-0.229	-0.191	0.029	6.615	1/2	30 300(5500)
^{172}Yb	1.76	0–6	33	-1.572	-1.237	0.037	8.019	0–1	173 000(14 000)
^{173}Yb	1.13	1/2–9/2	16	-0.363	-0.820	0.042	6.367	1/2	14 200(530)
^{174}Yb	1.64	0–4	11	-1.566	-1.686	0.080	7.465	2–3	128 000(15 000)
^{175}Yb	1.13	1/2–9/2	21	-0.377	-1.092	0.101	5.822	1/2	6200(700)
^{177}Yb	1.00	1/2–9/2	20	-0.299	-1.229	0.051	5.566	1/2	5400(560)
^{176}Lu	0.85	0–7	50	-1.310	-0.046	0.122	6.288	3–4	333 000(45 000)
^{177}Lu	0.96	1/2–9/2	15	-0.197	-0.601	0.104	7.073	13/2–15/2	364 000(112 000)
^{175}Hf	0.81	1/2–13/2	23	-0.179	0.025	0.055	6.708	1/2	55 600(15 400)
^{177}Hf	0.88	1/2–9/2	19	-0.121	-0.370	0.063	6.383	1/2	33 300(7800)
^{178}Hf	1.90	2–5	39	-1.282	-1.196	0.024	7.626	3–4	417 000(52 000)
^{179}Hf	1.29	1/2–9/2	36	-0.057	-0.676	-0.052	6.099	1/2	17 500(1800)
^{180}Hf	1.83	0–4	38	-1.400	-1.623	-0.011	7.388	4–5	217 000(14 000)
^{181}Hf	1.19	1/2–9/2	22	-0.232	-1.053	0.004	5.695	1/2	10 600(1700)
^{181}Ta	0.63	1/2–11/2	8	0.022	-0.809	-0.098	7.577	1/2–3/2	833 000(139 000)
^{182}Ta	0.79	2–5	39	-1.315	-0.332	-0.054	6.063	3–4	238 000(17 000)
^{183}Ta	0.98	5/2–7/2	14	-0.105	-0.900	-0.019	6.934	9/2–11/2	286 000(57 000)
^{181}W	0.96	1/2–7/2	15	-0.165	-0.621	-0.166	6.681	1/2	50 000(17 500)
^{183}W	1.24	1/2–9/2	23	-0.235	-1.067	-0.053	6.191	1/2	16 700(1700)
^{184}W	1.44	0–4	16	-1.526	-1.840	-0.034	7.412	0–1	83 300(6900)
^{185}W	1.25	1/2–9/2	46	-0.135	-1.129	-0.090	5.754	1/2	14 300(1400)
^{187}W	1.00	1/2–5/2	23	-0.218	-1.368	-0.156	5.467	1/2	11 800(1100)
^{186}Re	0.61	1–5	27	-1.492	-0.466	-0.101	6.179	2–3	323 000(31 000)
^{188}Re	0.56	1–5	30	-1.592	-0.740	-0.196	5.872	2–3	244 000(18 000)
^{187}Os	0.67	1/2–11/2	22	-0.081	-1.085	-0.032	6.290	1/2	34 500(3600)
^{188}Os	2.11	0–2	23	-1.796	-2.244	-0.032	7.990	0–1	250 000(38 000)
^{189}Os	0.61	1/2–7/2	17	-0.024	-1.506	-0.152	5.920	1/2	21 300(2700)
^{190}Os	1.48	0–6	17	-1.782	-2.809	-0.186	7.792	1–2	294 000(35 000)
^{191}Os	0.64	1/2–9/2	25	-0.138	-2.245	-0.322	5.759	1/2	14 300(2000)
^{193}Os	0.55	1/2–7/2	11	-0.373	-3.234	-0.420	5.583	1/2	8700(800)
^{192}Ir	0.46	0–3	32	-1.902	-1.483	-0.330	6.198	1–2	400 000(80 000)
^{193}Ir	1.09	1/2–7/2	28	-0.061	-2.837	-0.368	7.772	1/2	1 429 000(408 000)
^{194}Ir	0.55	0–3	35	-1.735	-2.649	-0.411	6.067	1–2	142 900(40 800)
^{193}Pt	0.54	1/2–7/2	15	0.161	-2.449	-0.411	6.255	1/2	45 500(17 000)
^{195}Pt	0.70	1/2–7/2	20	0.041	-3.719	-0.504	6.105	1/2	5000(2000)
^{196}Pt	2.01	0–6	32	-1.592	-5.292	-0.568	7.922	0–1	55 600(9300)
^{197}Pt	0.60	1/2–7/2	14	-0.030	-4.949	-0.608	5.846	1/2	2860(820)
^{199}Pt	0.65	1/2–7/2	12	-0.058	-6.157	-0.694	5.556	1/2	2940(780)
^{198}Au	0.68	0–3	26	-1.494	-4.920	-0.603	6.512	1–2	60 600(3300)
^{199}Hg	0.76	1/2–5/2	10	-0.385	-6.211	-0.528	6.664	1/2	9500(3200)
^{200}Hg	2.20	0–2	21	-1.721	-7.703	-0.572	8.028	0–1	12 500(4700)
^{201}Hg	0.65	1/2–7/2	11	-0.235	-7.556	-0.592	6.230	1/2	1540(360)
^{202}Hg	1.87	0–4	24	-1.538	-9.090	-0.648	7.754	1–2	11 100(3700)
^{204}Tl	0.69	0–4	15	-1.220	-8.932	-0.573	6.656	0–1	3600(640)
^{206}Tl	2.00	0–6	24	-0.966	-10.818	-0.634	6.504	0–1	182(50)
^{205}Pb	2.26	1/2–9/2	29	-0.862	-9.699	-0.165	6.732	1/2	500(125)
^{207}Pb	2.74	1/2–9/2	8	-1.412	-11.869	-0.110	6.738	1/2	31(6)
^{208}Pb	4.37	0–8	24	-3.226	-13.137	0.411	7.368	0–1	26(6)

TABLE I. (Continued.)

Nucleus	Energy range (MeV)	Spin window (\hbar)	Number of levels	Deuteron pairing ^a (MeV)	Shell energy ^b (MeV)	Δ Shell energy ^c (MeV)	n binding energy (MeV)	Spin (\hbar)	Density (per MeV)
^{209}Pb	3.69	1/2–15/2	40	-1.168	-11.126	0.886	3.937	1/2	3(1)
^{210}Bi	1.48	2–7	19	-1.267	-9.173	1.307	4.605	4–5	250(44)
^{227}Ra	0.53	1/2–5/2	16	-0.105	1.271	0.093	4.561	1/2	32 300(6300)
^{229}Th	0.49	1/2–7/2	20	-0.052	1.147	-0.001	5.257	1/2	200 000(120 000)
^{230}Th	1.20	0–5	24	-1.558	0.306	-0.089	6.794	2–3	1 613 000(312 000)
^{231}Th	0.99	1/2–5/2	30	-0.305	1.006	-0.125	5.118	1/2	104 000(16 000)
^{233}Th	0.79	1/2–5/2	24	-0.391	1.019	-0.118	4.786	1/2	60 200(2200)
^{233}Pa	0.48	1/2–11/2	30	-0.121	0.979	-0.115	6.529	3/2–5/2	1 330 000(270 000)
^{234}Pa	0.20	0–4	8	-1.394	1.530	-0.099	5.220	1–2	1 670 000(280 000)
^{233}U	0.63	1/2–9/2	20	-0.315	0.575	-0.152	5.762	1/2	217 000(33 000)
^{234}U	1.50	0–6	39	-1.517	-0.147	-0.157	6.845	2–3	1 818 000(165 000)
^{235}U	0.90	1/2–5/2	22	-0.261	0.545	-0.127	5.297	1/2	83 300(5600)
^{236}U	1.17	0–6	26	-1.452	-0.144	-0.152	6.545	3–4	2 326 000(108 000)
^{237}U	0.77	1/2–5/2	12	-0.430	0.456	-0.143	5.126	1/2	66 700(4500)
^{238}U	1.27	0–4	25	-1.522	-0.100	-0.103	6.154	0–1	286 000(65 000)
^{239}U	0.97	1/2–5/2	20	-0.378	0.562	-0.147	4.806	1/2	48 100(700)
^{237}Np	0.87	1/2–11/2	35	-0.118	0.470	-0.137	6.580	1/2–3/2	1 670 000(170 000)
^{238}Np	0.40	1–5	29	-1.170	0.923	-0.092	5.488	2–3	1 754 000(92 000)
^{239}Np	0.53	1/2–11/2	23	-0.138	0.519	-0.079	6.215	3/2–5/2	2 440 000(600 000)
^{239}Pu	0.91	1/2–9/2	24	-0.315	-0.001	-0.119	5.646	1/2	111 000(12 000)
^{240}Pu	1.25	0–5	24	-1.336	-0.512	-0.090	6.534	0–1	455 000(10 000)
^{241}Pu	0.85	1/2–9/2	24	-0.287	0.141	-0.086	5.242	1/2	80 600(4600)
^{242}Pu	1.19	0–4	14	-1.379	-0.402	-0.118	6.310	0–1	1 370 000(150 000)
^{243}Pu	0.91	1/2–9/2	25	-0.325	0.202	-0.058	5.034	1/2	74 000(8200)
^{245}Pu	0.58	1/2–9/2	8	-0.409	0.314	-0.123	4.771	1/2	52 600(8300)
^{242}Am	0.46	0–6	35	-1.179	0.565	-0.092	5.538	2–3	1 724 000(119 000)
^{243}Am	0.54	1/2–13/2	18	-0.195	0.176	-0.120	6.365	1/2–3/2	2 500 000(500 000)
^{244}Am	0.59	0–4	42	-1.213	0.659	-0.116	5.366	2–3	1 370 000(113 000)
^{243}Cm	0.98	1/2–9/2	21	-0.192	-0.265	-0.074	5.693	1/2	71 400(15 300)
^{244}Cm	1.19	0–3	8	-1.265	-0.878	-0.129	6.801	2–3	1 333 000(267 000)
^{245}Cm	0.80	1/2–11/2	26	-0.329	-0.340	-0.134	5.520	1/2	84 700(8600)
^{246}Cm	1.72	0–3	32	-1.362	-0.867	-0.134	6.458	0–1	769 000(118 000)
^{247}Cm	0.56	1/2–9/2	14	-0.341	-0.217	-0.143	5.156	1/2	33 300(5600)
^{248}Cm	1.31	0–4	12	-1.581	-0.750	-0.100	6.213	4–5	714 000(150 000)
^{249}Cm	0.59	1/2–9/2	18	-0.441	0.094	-0.001	4.713	1/2	35 700(6400)
^{250}Bk	0.24	1–6	20	-1.238	0.549	-0.010	4.970	3–4	909 000(83 000)
^{250}Cf	1.30	0–5	19	-1.515	-1.321	-0.016	6.625	4–5	1 429 000(204 000)
^{251}Cf	0.70	1/2–11/2	25	-0.297	-0.462	-0.001	5.108	1/2	83 300(14 000)

^aThe deuteron pairing energy, from mass table.^bShell correction, Eqs. (7) and (9).^cThe derivative of $S(Z, N)$ with respect to the mass, calculated with Eq. (12).

spacings $D(U, J_1, J_2) = 1/\rho(U, J_1, J_2)$ in a spin window from J_1 to J_2 [where $\rho(U, J_1, J_2) = \sum_{J_1}^{J_2} \rho(U, J)$] are fitted to the experimental spacings $S_i = (U_{i+1} - U_i)$, including the average neutron resonance spacing D_{res} . For each nucleus, the following χ^2 quantity has been minimized:

$$\chi^2 = \sum_i [(S_i - D_i)W_i]^2 + \{[D_{\text{res}} - D(B_n, J_{\text{res}})]/\Delta D_{\text{res}}\}^2.$$

The weight W_i of the experimental spacings of adjacent levels is given by the spacing distribution, i.e., the fluctuation of level distances. The spacing of levels with different spins and

parities follows a Poisson (exponential) distribution [11],

$$P(S/D) = e^{-S/D},$$

because the different quantum numbers prevent correlations between levels. The average value of an exponential function is 1, and the fluctuations correspond to the level spacing D_i . Consequently,

$$W_i = 1/D_i.$$

However, W_i is not varied in the fit procedure, because this would give a tendency toward too large D_i . Therefore the fit procedure was repeated about four times and the weight was

adjusted each time to the previously fitted D_i ; this converged easily.

Usually one determines the low-energy LD either by counting levels in arbitrary energy bins or by fitting the density function to the accumulated number of levels. Compared with these methods, our fit to each individual level spacing has essential advantages because we do not need arbitrary binning, the weight at very low energies for which special nuclear structures play a role is small, and we obtain automatically the correct errors of the LD parameters.

In general, for all the considered models, good fits have been obtained, with χ^2 values close to 1; therefore all three models give a good description to both the low-energy LD and the average neutron resonance density.

Table II gives the model parameters obtained from the fit, which are examined in the rest of the paper.

We emphasize here the main difference between our procedure and other approaches that also determine phenomenological parameters for the formulas just outlined. As already said, there are many sets of LD parameters based on only the neutron resonance LDs. To fit such data, very often one of the two model parameters has been eliminated (fixed to some values), leaving only one for the fit. Usually it has been assumed that the energy shifts (or backshifts) E_i were due only to the pairing; therefore they were related to the neutron and proton pairing energies P_n and P_p , respectively. Thus, in many applications, the backshifts are kept fixed at values related to assumed pairing energies. A rough approximation is the simple functional dependence of the pairing gap $\delta = 12/\sqrt{A}$. Thus, in Ref. [10], the backshifts are chosen as $\chi 12/\sqrt{A}$, with $\chi = 0, 1, 2$, for the odd-odd, odd-even, and even-even nuclei, respectively. Other descriptions are obtained by use of pairing energies from the mass tables, like $1/2(P_p + P_n)$ (for even-even nuclei), $-1/2(P_p + P_n)$ (for odd-odd), and 0 (for odd- A) [9], or, as found empirically [14], $-1/3P_n(P_p)$ [for odd- $Z(N)$ nuclei]. Relating the backshifts to the nucleon pairing implies putting all the shell effects in the second parameter of the model (e.g., a in the case of the BSFG model). Nevertheless, it is not *a priori* obvious that the backshifts must depend only on the pairing. From this point of view, our procedure of leaving free in the fit both model parameters appears justified. Of course, the phenomenological values obtained in this way will have an increased usefulness if one succeeds in understanding and systematizing their behavior. It should be mentioned that other recent publications used also for LD calculations the experimental low-energy level schemes and determined shell corrections in a way similar to that already mentioned [14,15].

III. SYSTEMATICS OF THE LD PARAMETERS

A. Results of the fits to the experimental LDs

Figure 1 shows, as an example, the quality of the BSFG and CT fits to the experimental cumulative number of levels of ^{26}Al , one of the light nuclei with a complete level scheme in the spin range $0-5\hbar$, up to 8.2-MeV excitation. Figure 2 displays the results of the fits to the experimental data of Table I with

the three two-parameter models: namely, the variation with the mass number of the parameters a and E_1 of the BSFG model; \tilde{a} and E_2 of the BSFG model with energy dependence (BSFG-ED); and T and E_0 of the CT model.

These empirically determined parameters have, generally, a complicated behavior. We note the following empirical observations. The parameters a , \tilde{a} , and T do not show notable dependence on the type of nucleus (even-even, odd- A , or odd-odd). a shows a strong dependence on shell effects, having large variations at the shell closures, as observed in many other similar parameter sets (see, e.g., Refs. [1,10]). Similarly, T shows strong variations at the shell closures. The parameter \tilde{a} is rather similar to that of other comparable evaluations [7,10], although its absolute values correspond to our particular approach; the shell effects have almost disappeared in this parameter, because of the way they were incorporated in formula (5).

The backshift energies E_1 , E_2 , and E_0 have an even more complicated behavior, and in addition present a dependence on the type of the nucleus. In general, they are positive for the even-even nuclei, negative for the odd-odd nuclei, and smaller and negative for the odd- A nuclei, for which they also show some notable oscillations. We note, however, that the behavior of these parameters is very similar for all three models: E_1 and E_2 are almost identical, and there is a practically linear correlation between E_0 and E_1 (or E_2): Fig. 3 shows these correlations between E_2 and E_1 , as well as between E_0 and E_1 .

B. Fits of the LD parameters as functions of various nuclear properties

It was tried to reproduce the deduced LD parameters by simple formulas with various values obtained from atomic masses and other tabulated experimental nuclear properties. For each LD parameter (a , E_1 , \tilde{a} , E_2 , T , E_0) a least-squares program was written and a large variety of functions were fitted to the corresponding experimental parameters of the 310 nuclides. Even-even, odd, and odd-odd nuclei were frequently treated separately. Linear, quadratic, logarithmic, etc., dependencies were tried, but simple functions with few variables were preferred. In this way hundreds of χ^2 values were produced and compared. The results of careful evaluations of all these calculations are presented in the following subsections. Only the best results are given. The obtained normalized χ^2 values lie between 2 and 4.

C. Correlations of a , \tilde{a} , and T with shell and pairing effects

As observed a long time ago [3], and in many more recent publications, the LD parameter a (Fig. 2) shows an almost linear dependence on A and a clear correlation with the shell correction S [Eq. (7)], having minima at the shell closures, where S is negative. This allowed a description of this parameter in terms of a simple formula of the type $a/A = c_0 + c_1 S(Z, N)$ [3], with the two constants c_0 and c_1 suitably chosen. Indeed, the data shown in Fig. 2 can be described reasonably well by such a formula. The parameter

TABLE II. LD parameters for the three models determined from fits to the data specified by Table I.

Nucleus	BSFG		BSFG with ED		CT	
	$a(\delta a)$ (MeV $^{-1}$)	$E_1(\delta E_1)$ (MeV)	$\tilde{a}(\delta \tilde{a})$ (MeV $^{-1}$)	$E_2(\delta E_2)$ (MeV)	$T(\delta T)$ (MeV)	$E_0(\delta E_0)$ (MeV)
^{18}F	2.68(47)	-1.28(174)	2.88(53)	-1.49(182)	2.33(43)	-2.37(186)
^{19}F	2.26(36)	-2.52(199)	2.13(32)	-2.25(189)	2.84(50)	-3.57(223)
^{20}F	2.86(34)	-2.16(133)	2.65(30)	-1.98(128)	2.23(45)	-3.49(206)
^{20}Ne	2.24(26)	1.46(165)	2.31(28)	1.32(167)	2.94(33)	0.29(158)
^{23}Na	3.11(40)	0.46(130)	3.09(39)	0.47(129)	2.19(28)	-1.03(135)
^{24}Na	2.99(31)	-2.41(110)	2.88(29)	-2.30(108)	2.20(62)	-3.40(277)
^{24}Mg	3.04(47)	3.71(151)	3.35(51)	3.80(140)	2.37(30)	1.75(134)
^{25}Mg	3.23(37)	0.39(108)	3.28(37)	0.37(108)	2.24(32)	-1.47(145)
^{26}Mg	3.32(39)	1.37(103)	3.28(38)	1.40(103)	2.05(28)	0.20(129)
^{27}Mg	4.58(45)	1.61(68)	4.42(43)	1.63(68)	1.46(21)	0.33(94)
^{26}Al	2.90(28)	-2.91(120)	3.16(34)	-3.34(131)	2.43(23)	-4.38(133)
^{27}Al	3.02(44)	-0.57(144)	3.16(46)	-0.75(147)	2.19(33)	-1.29(148)
^{28}Al	3.60(22)	-1.31(70)	3.67(22)	-1.37(71)	1.98(19)	-2.69(108)
^{28}Si	3.43(55)	4.38(115)	4.14(69)	4.30(124)	2.04(24)	3.12(105)
^{29}Si	3.87(46)	2.30(87)	4.37(58)	1.97(100)	2.16(27)	-0.48(131)
^{30}Si	2.73(29)	-0.62(152)	2.87(31)	-0.71(148)	2.49(34)	-1.05(167)
^{30}P	3.21(32)	-1.31(110)	3.74(43)	-1.86(126)	2.14(25)	-2.17(124)
^{31}P	3.58(66)	0.47(149)	4.01(76)	0.24(155)	1.84(33)	-0.12(139)
^{32}P	3.75(29)	-1.21(74)	3.95(31)	-1.34(76)	2.00(35)	-2.79(167)
^{32}S	3.39(63)	1.65(17)	3.95(80)	1.34(183)	1.97(34)	1.06(142)
^{33}S	4.01(26)	0.25(62)	4.36(29)	0.11(64)	1.75(24)	-0.56(112)
^{34}S	3.94(32)	1.32(73)	4.09(34)	1.22(75)	1.84(25)	0.30(114)
^{35}S	4.50(55)	0.12(93)	4.43(54)	0.14(93)	1.50(25)	-0.52(114)
^{36}Cl	4.19(30)	-1.06(74)	4.28(31)	-1.11(75)	1.85(29)	-2.61(151)
^{38}Cl	6.14(57)	-0.09(70)	5.61(52)	-0.04(69)	1.17(15)	-1.01(87)
^{38}Ar	4.21(59)	1.36(107)	4.21(59)	1.35(107)	1.51(18)	1.30(80)
^{40}Ar	4.72(81)	0.54(110)	4.18(69)	0.65(104)	1.35(22)	0.43(92)
^{41}Ar	5.78(53)	-0.27(75)	4.95(44)	-0.02(72)	1.32(18)	-1.54(102)
^{40}K	4.73(23)	-1.54(58)	4.60(22)	-1.47(57)	1.66(22)	-2.93(131)
^{41}K	5.61(11)	-0.13(26)	5.10(9)	0.05(24)	1.43(8)	-1.64(60)
^{42}K	4.40(37)	-3.03(85)	3.94(31)	-2.79(79)	1.85(26)	-4.58(147)
^{40}Ca	5.27(74)	3.61(87)	5.29(88)	2.88(112)	1.45(20)	2.28(89)
^{41}Ca	5.65(20)	0.50(35)	5.69(20)	0.49(35)	1.30(10)	-0.20(62)
^{43}Ca	5.77(35)	-0.69(53)	5.23(30)	-0.56(50)	1.38(13)	-1.96(80)
^{44}Ca	5.93(27)	1.06(49)	5.36(23)	1.18(47)	1.34(8)	-0.03(61)
^{45}Ca	6.38(30)	0.13(44)	5.70(26)	0.22(43)	1.23(9)	-1.02(63)
^{46}Sc	5.82(14)	-2.22(34)	5.41(13)	-2.08(32)	1.44(10)	-3.77(76)
^{47}Ti	5.14(30)	-1.35(74)	4.96(28)	-1.26(72)	1.65(16)	-2.94(110)
^{48}Ti	5.67(20)	0.59(42)	5.47(19)	0.66(41)	1.47(8)	-0.73(60)
^{49}Ti	6.36(31)	0.07(49)	6.18(30)	0.10(49)	1.25(10)	-0.89(70)
^{50}Ti	6.06(33)	2.13(50)	6.02(33)	2.14(50)	1.30(8)	1.19(58)
^{51}Ti	5.74(85)	0.11(87)	5.72(84)	0.11(87)	1.29(24)	-0.55(100)
^{51}V	7.06(29)	0.93(35)	7.15(30)	0.92(35)	1.23(7)	-0.37(50)
^{52}V	6.34(29)	-0.94(39)	6.36(29)	-0.94(39)	1.23(8)	-1.76(57)
^{51}Cr	5.91(18)	-0.41(38)	6.20(20)	-0.49(39)	1.42(8)	-1.68(61)
^{53}Cr	5.66(26)	-0.46(55)	5.88(27)	-0.53(56)	1.46(12)	-1.60(80)
^{54}Cr	5.73(24)	0.60(51)	5.77(24)	0.59(51)	1.44(9)	-0.48(68)
^{55}Cr	6.30(27)	-0.49(41)	6.11(26)	-0.45(41)	1.27(14)	-1.45(78)
^{56}Mn	6.28(30)	-2.31(45)	6.35(31)	-2.33(46)	1.39(10)	-3.94(69)
^{55}Fe	5.73(22)	-0.62(54)	6.56(29)	-0.94(59)	1.49(14)	-1.84(94)
^{57}Fe	5.92(19)	-1.34(36)	6.25(21)	-1.45(37)	1.47(9)	-2.83(61)
^{58}Fe	6.26(24)	0.55(42)	6.37(25)	0.52(42)	1.37(8)	-0.62(60)
^{59}Fe	6.75(37)	-0.91(45)	6.64(36)	-0.89(44)	1.24(11)	-2.00(68)
^{60}Co	7.23(19)	-1.37(25)	7.41(20)	-1.40(25)	1.1(8)	-2.61(55)
^{59}Ni	6.10(21)	-0.84(47)	7.11(28)	-1.19(53)	1.43(9)	-2.10(72)
^{60}Ni	6.05(40)	0.28(61)	6.69(46)	0.08(65)	1.44(12)	-0.85(77)

TABLE II. (*Continued.*)

Nucleus	BSFG		BSFG with ED		CT	
	$a(\delta a)$ (MeV $^{-1}$)	$E_1(\delta E_1)$ (MeV)	$\tilde{a}(\delta \tilde{a})$ (MeV $^{-1}$)	$E_2(\delta E_2)$ (MeV)	$T(\delta T)$ (MeV)	$E_0(\delta E_0)$ (MeV)
^{61}Ni	6.79(16)	-0.69(29)	7.23(18)	-0.79(30)	1.28(8)	-1.96(60)
^{62}Ni	6.52(21)	0.54(43)	6.70(22)	0.50(44)	1.33(7)	-0.48(60)
^{63}Ni	7.08(38)	-1.08(51)	7.05(38)	-1.07(51)	1.20(11)	-2.11(77)
^{65}Ni	8.31(40)	-0.03(38)	7.85(41)	-0.04(43)	1.03(8)	-1.20(58)
^{64}Cu	7.26(22)	-1.99(36)	7.35(22)	-2.02(37)	1.27(7)	-3.64(58)
^{66}Cu	8.01(23)	-1.28(29)	7.69(21)	-1.22(28)	1.12(5)	-2.70(45)
^{65}Zn	7.86(23)	-0.91(36)	7.83(23)	-0.91(36)	1.16(6)	-2.32(56)
^{67}Zn	8.30(24)	-0.95(29)	7.76(22)	-0.88(29)	1.07(8)	-2.16(60)
^{68}Zn	8.42(26)	1.14(30)	7.88(24)	1.21(30)	1.05(5)	0.13(41)
^{69}Zn	9.03(29)	-0.50(31)	8.15(25)	-0.41(29)	0.98(6)	-1.67(47)
^{71}Zn	10.14(49)	0.09(38)	8.96(42)	0.22(38)	0.87(7)	-1.03(49)
^{70}Ga	10.09(37)	-0.66(25)	9.22(33)	-0.59(24)	0.91(5)	-1.81(41)
^{72}Ga	9.91(31)	-1.23(23)	8.77(26)	-1.13(22)	0.92(5)	-2.44(39)
^{71}Ge	9.82(40)	-0.91(23)	8.76(35)	-0.80(22)	0.95(5)	-2.29(38)
^{73}Ge	9.67(33)	-1.15(23)	8.40(27)	-1.04(22)	0.95(5)	-2.35(40)
^{74}Ge	9.96(34)	0.77(21)	8.82(30)	0.88(20)	0.91(4)	-0.29(30)
^{75}Ge	9.14(55)	-1.16(29)	8.06(48)	-1.06(28)	0.98(8)	-2.28(47)
^{77}Ge	9.29(53)	-1.15(33)	8.52(48)	-1.09(32)	0.96(8)	-2.14(53)
^{76}As	10.39(20)	-1.89(18)	9.21(17)	-1.75(17)	0.96(3)	-3.59(32)
^{75}Se	10.12(30)	-1.25(21)	8.95(25)	-1.12(20)	0.96(6)	-2.77(49)
^{77}Se	10.10(26)	-1.18(25)	8.86(22)	-1.06(23)	0.94(6)	-2.50(53)
^{78}Se	10.25(34)	0.75(18)	9.13(30)	0.84(17)	0.93(4)	-0.32(29)
^{79}Se	9.41(39)	-1.15(24)	8.41(34)	-1.04(23)	0.99(6)	-2.37(41)
^{81}Se	10.83(35)	-0.06(21)	10.22(33)	-0.01(21)	0.83(4)	-1.00(32)
^{83}Se	10.09(42)	-0.71(31)	10.12(42)	-0.71(31)	0.90(6)	-1.76(47)
^{80}Br	10.65(19)	-1.74(17)	9.62(17)	-1.62(16)	0.94(3)	-3.37(30)
^{82}Br	10.70(26)	-1.12(20)	10.10(24)	-1.07(19)	0.90(4)	-2.34(34)
^{79}Kr	10.29(41)	-1.22(20)	9.22(36)	-1.12(19)	0.95(5)	-2.62(35)
^{81}Kr	11.17(34)	-0.66(20)	10.03(30)	-0.57(19)	0.87(4)	-1.91(34)
^{84}Kr	8.93(32)	0.97(28)	8.74(31)	0.99(28)	0.98(4)	0.25(37)
^{85}Kr	12.47(37)	0.87(15)	12.48(38)	0.87(50)	0.73(3)	-0.02(22)
^{86}Rb	9.53(26)	-0.64(22)	9.85(27)	-0.67(22)	0.99(4)	-1.71(35)
^{88}Rb	9.81(36)	-0.54(25)	10.34(39)	-0.59(25)	0.91(5)	-1.39(37)
^{85}Sr	10.93(54)	-0.18(21)	10.48(52)	-0.14(20)	0.88(5)	-1.30(33)
^{87}Sr	9.11(44)	-0.10(38)	9.43(46)	-0.16(38)	1.04(11)	1.28(74)
^{88}Sr	8.95(41)	1.97(30)	9.71(45)	1.88(31)	0.97(5)	1.31(37)
^{89}Sr	9.63(39)	0.87(28)	10.51(44)	0.80(29)	0.88(6)	0.25(39)
^{90}Y	9.03(32)	-0.57(33)	9.81(36)	-0.67(34)	1.01(6)	-1.48(48)
^{91}Zr	10.03(44)	0.52(25)	11.05(50)	0.39(26)	0.89(5)	-0.23(36)
^{92}Zr	9.99(34)	1.07(25)	10.47(36)	1.03(25)	0.90(4)	0.29(33)
^{93}Zr	10.72(52)	0.10(33)	10.95(53)	0.08(33)	0.86(6)	-0.85(45)
^{94}Zr	12.02(46)	1.13(31)	11.86(45)	1.16(31)	0.76(4)	0.35(36)
^{95}Zr	11.89(63)	0.59(31)	11.63(61)	0.60(31)	0.76(5)	-0.19(40)
^{97}Zr	11.77(66)	0.81(30)	11.06(61)	0.83(29)	0.71(5)	0.38(37)
^{94}Nb	10.88(26)	-1.37(20)	11.07(27)	-1.39(21)	0.86(3)	-2.44(33)
^{93}Mo	9.78(34)	0.21(26)	11.31(41)	0.08(27)	0.94(5)	-0.60(38)
^{95}Mo	10.56(29)	-0.52(28)	11.04(31)	-0.56(29)	0.89(6)	-1.41(51)
^{96}Mo	10.90(21)	0.59(21)	10.88(21)	0.60(21)	0.87(4)	-0.29(35)
^{97}Mo	11.14(36)	-0.81(21)	10.83(35)	-0.78(21)	0.87(4)	-1.91(34)
^{98}Mo	12.02(41)	0.68(16)	11.29(38)	0.72(16)	0.79(3)	-0.18(25)
^{99}Mo	12.57(41)	-0.64(17)	11.37(36)	-0.58(17)	0.75(4)	-1.53(29)
^{101}Mo	13.00(40)	-1.11(16)	11.21(33)	-1.02(15)	0.74(3)	-2.17(27)
^{100}Tc	13.93(31)	-1.26(15)	12.95(29)	-1.21(14)	0.71(3)	-2.44(25)
^{100}Ru	12.15(26)	0.70(15)	12.00(25)	0.72(16)	0.80(2)	-0.16(25)
^{102}Ru	12.94(27)	0.57(19)	12.04(25)	0.62(19)	0.76(3)	-0.30(32)
^{103}Ru	12.30(48)	-1.18(18)	11.11(43)	-1.12(18)	0.80(4)	-2.27(32)

TABLE II. (*Continued.*)

Nucleus	BSFG		BSFG with ED		CT	
	$a(\delta a)$ (MeV $^{-1}$)	$E_1(\delta E_1)$ (MeV)	$\tilde{a}(\delta \tilde{a})$ (MeV $^{-1}$)	$E_2(\delta E_2)$ (MeV)	$T(\delta T)$ (MeV)	$E_0(\delta E_0)$ (MeV)
^{105}Ru	13.39(51)	-1.31(21)	11.81(44)	-1.21(20)	0.75(4)	-2.55(34)
^{104}Rh	13.33(22)	-1.75(15)	12.50(20)	-1.68(14)	0.81(4)	-3.38(39)
^{105}Pd	12.79(26)	-0.81(16)	12.35(25)	-0.79(16)	0.78(3)	-1.88(28)
^{106}Pd	13.42(16)	0.68(14)	12.71(15)	0.73(14)	0.75(2)	-0.29(26)
^{107}Pd	13.46(56)	-0.77(19)	12.37(51)	-0.73(18)	0.72(4)	-1.63(32)
^{108}Pd	14.34(22)	1.07(14)	13.09(19)	1.13(14)	0.70(2)	0.18(21)
^{109}Pd	14.02(34)	-1.19(18)	12.60(30)	-1.11(17)	0.72(5)	-2.34(40)
^{111}Pd	15.84(66)	-0.71(16)	14.05(57)	-0.66(16)	0.62(4)	-1.56(28)
^{108}Ag	14.27(29)	-1.18(14)	13.68(27)	-1.15(14)	0.74(4)	-2.47(34)
^{110}Ag	14.93(19)	-1.55(12)	13.85(17)	-1.48(11)	0.73(3)	-3.10(32)
^{107}Cd	12.84(42)	-0.51(17)	13.54(45)	-0.55(17)	0.79(3)	-1.63(28)
^{109}Cd	14.04(45)	-0.33(16)	13.92(45)	-0.33(16)	0.72(3)	-1.36(26)
^{111}Cd	14.04(27)	-0.52(13)	13.43(26)	-0.49(13)	0.72(2)	-1.64(22)
^{112}Cd	14.25(30)	0.77(18)	13.50(29)	0.81(17)	0.71(3)	-0.06(30)
^{113}Cd	14.17(29)	-0.74(13)	13.25(26)	-0.69(12)	0.72(2)	-1.90(22)
^{114}Cd	14.73(20)	0.92(12)	13.81(18)	0.99(12)	0.71(2)	-0.23(23)
^{115}Cd	15.06(35)	-0.43(13)	14.01(32)	-0.39(13)	0.66(2)	-1.37(22)
^{117}Cd	15.27(53)	-0.25(15)	14.41(49)	-0.22(15)	0.63(3)	-1.04(24)
^{114}In	14.23(38)	-0.68(19)	13.84(37)	-0.67(19)	0.69(4)	-1.52(38)
^{116}In	14.76(23)	-1.12(16)	14.22(21)	-1.09(16)	0.69(4)	-2.26(36)
^{113}Sn	13.67(56)	-0.03(18)	14.16(59)	-0.06(18)	0.74(4)	-1.06(27)
^{115}Sn	14.07(68)	0.52(25)	14.37(70)	0.51(25)	0.70(4)	-0.33(33)
^{116}Sn	14.13(40)	1.66(11)	13.99(40)	1.67(11)	0.73(2)	0.52(17)
^{117}Sn	14.15(66)	0.21(18)	14.16(66)	0.21(18)	0.69(4)	-0.68(27)
^{118}Sn	13.53(27)	0.96(20)	13.33(26)	0.97(20)	0.74(3)	0.21(30)
^{119}Sn	14.38(42)	0.05(15)	14.42(42)	0.04(15)	0.68(3)	-0.85(23)
^{120}Sn	13.14(40)	0.85(22)	13.17(40)	0.85(22)	0.76(3)	0.12(32)
^{121}Sn	12.23(35)	-0.66(22)	12.63(37)	-0.69(23)	0.79(4)	-1.47(34)
^{123}Sn	12.84(62)	-0.47(24)	14.07(70)	-0.54(25)	0.74(5)	-1.20(36)
^{125}Sn	12.10(58)	-0.20(27)	14.44(73)	-0.36(28)	0.77(5)	-0.83(37)
^{122}Sb	14.78(29)	-1.13(16)	14.90(30)	-1.14(16)	0.70(4)	-2.21(35)
^{124}Sb	14.14(25)	-1.22(14)	14.94(27)	-1.26(15)	0.71(3)	-2.25(32)
^{123}Te	15.12(26)	-0.21(11)	14.84(25)	-0.20(11)	0.68(2)	-1.27(18)
^{124}Te	15.04(30)	1.00(11)	15.10(31)	1.00(11)	0.71(2)	-0.10(18)
^{125}Te	15.51(25)	-0.07(9)	15.80(26)	-0.10(9)	0.67(2)	-1.19(15)
^{126}Te	14.36(24)	0.88(10)	15.17(26)	0.85(11)	0.72(2)	-0.08(17)
^{127}Te	13.89(40)	-0.44(13)	15.08(44)	-0.51(14)	0.73(3)	-1.50(21)
^{129}Te	14.21(47)	-0.18(14)	16.96(59)	-0.33(15)	0.69(3)	-1.09(22)
^{131}Te	14.18(43)	0.17(15)	19.36(65)	-0.08(17)	0.68(3)	-0.63(22)
^{128}I	14.01(33)	-1.64(17)	14.81(36)	-1.70(18)	0.76(5)	-2.89(41)
^{130}I	12.87(25)	-2.07(21)	14.52(31)	-2.23(22)	0.81(5)	-3.34(50)
^{129}Xe	13.39(68)	-0.94(21)	13.84(71)	-0.97(21)	0.76(5)	-1.88(34)
^{130}Xe	14.05(25)	0.73(14)	14.94(27)	0.68(14)	0.73(2)	-0.08(22)
^{131}Xe	14.41(51)	-0.66(20)	15.85(58)	-0.73(21)	0.70(4)	-1.50(32)
^{132}Xe	13.50(55)	0.95(16)	15.49(63)	0.84(17)	0.75(3)	0.08(24)
^{133}Xe	13.37(62)	-0.48(24)	16.15(80)	-0.63(26)	0.73(5)	-1.18(36)
^{135}Xe	14.15(81)	0.58(20)	19.86(119)	0.36(22)	0.68(5)	-0.12(26)
^{137}Xe	15.71(44)	0.38(25)	23.37(225)	0.23(27)	0.54(6)	-0.03(29)
^{134}Cs	13.37(22)	-1.65(16)	15.28(27)	-1.81(18)	0.78(4)	-2.82(37)
^{135}Cs	12.50(40)	-0.77(33)	14.86(54)	-0.97(36)	0.80(4)	-1.50(51)
^{131}Ba	14.90(36)	-0.65(17)	14.89(35)	-0.65(17)	0.71(3)	-1.72(27)
^{133}Ba	14.44(59)	-0.72(20)	15.04(62)	-0.75(20)	0.72(4)	-1.73(31)
^{135}Ba	13.11(40)	-0.86(30)	14.58(47)	-0.96(32)	0.77(4)	-1.66(46)
^{136}Ba	13.49(30)	0.69(17)	15.65(37)	0.57(19)	0.75(3)	-0.03(27)
^{137}Ba	13.58(34)	0.45(20)	16.85(47)	0.29(21)	0.72(3)	-0.25(28)
^{138}Ba	12.39(39)	1.12(22)	15.60(54)	0.88(24)	0.79(3)	0.48(30)

TABLE II. (*Continued.*)

Nucleus	BSFG		BSFG with ED		CT	
	$a(\delta a)$ (MeV $^{-1}$)	$E_1(\delta E_1)$ (MeV)	$\tilde{a}(\delta \tilde{a})$ (MeV $^{-1}$)	$E_2(\delta E_2)$ (MeV)	$T(\delta T)$ (MeV)	$E_0(\delta E_0)$ (MeV)
^{139}Ba	12.69(65)	0.04(29)	16.05(90)	-0.14(32)	0.72(6)	-0.48(41)
^{139}La	12.27(34)	-0.22(23)	14.87(45)	-0.47(25)	0.79(3)	-0.83(32)
^{140}La	13.52(40)	-1.20(19)	16.17(51)	-1.35(21)	0.71(5)	-1.91(38)
^{137}Ce	16.30(67)	-0.01(15)	17.18(76)	-0.08(17)	0.65(3)	-0.91(26)
^{141}Ce	15.39(51)	0.62(17)	18.08(63)	0.55(18)	0.60(3)	0.11(24)
^{142}Ce	15.48(58)	0.90(16)	17.34(66)	0.83(17)	0.62(4)	0.22(26)
^{143}Ce	15.83(99)	-0.25(20)	17.21(111)	-0.30(21)	0.61(7)	-0.84(41)
^{142}Pr	13.97(69)	-1.05(38)	15.73(82)	-1.14(40)	0.71(9)	-1.78(73)
^{143}Nd	15.54(38)	0.40(17)	17.37(44)	0.33(17)	0.64(3)	-0.36(26)
^{144}Nd	15.40(28)	0.95(12)	16.44(30)	0.91(12)	0.64(2)	0.29(20)
^{145}Nd	17.08(35)	0.25(11)	17.78(37)	0.23(12)	0.59(2)	-0.55(17)
^{146}Nd	16.12(38)	0.51(13)	16.25(38)	0.51(13)	0.63(2)	-0.25(19)
^{147}Nd	16.96(50)	-0.62(17)	16.63(49)	-0.61(17)	0.60(3)	-1.39(28)
^{148}Nd	19.70(103)	0.70(16)	18.90(98)	0.72(16)	0.53(3)	-0.07(22)
^{149}Nd	18.57(38)	-0.65(11)	17.51(35)	-0.62(11)	0.55(2)	-1.48(18)
^{151}Nd	17.26(34)	-0.91(14)	16.55(32)	-0.89(14)	0.60(2)	-1.76(24)
^{148}Pm	17.33(59)	-1.48(22)	16.79(56)	-1.45(22)	0.62(3)	-2.57(36)
^{145}Sm	14.82(28)	0.43(14)	16.38(32)	0.37(14)	0.66(2)	-0.19(21)
^{148}Sm	17.34(23)	0.77(9)	17.05(23)	0.78(9)	0.60(1)	-0.01(15)
^{149}Sm	17.95(44)	-0.39(11)	17.14(42)	-0.37(10)	0.57(2)	-1.12(18)
^{150}Sm	18.77(29)	0.64(8)	17.57(27)	0.66(8)	0.56(1)	-0.15(14)
^{151}Sm	18.55(41)	-0.98(14)	17.02(37)	-0.93(14)	0.59(4)	-2.08(34)
^{152}Sm	18.96(26)	0.45(10)	17.61(24)	0.48(10)	0.56(2)	-0.25(18)
^{153}Sm	17.76(28)	-1.08(13)	16.62(25)	-1.05(12)	0.61(3)	-2.06(29)
^{155}Sm	17.19(35)	-0.80(15)	16.77(33)	-0.79(15)	0.61(3)	-1.68(32)
^{152}Eu	19.62(20)	-1.60(8)	18.09(18)	-1.54(8)	0.60(2)	-3.03(22)
^{153}Eu	17.27(27)	-0.83(12)	15.98(24)	-0.78(11)	0.65(3)	-1.88(26)
^{154}Eu	19.13(31)	-1.43(8)	17.92(29)	-1.38(8)	0.60(3)	-2.77(22)
^{155}Eu	17.73(27)	-0.54(11)	16.87(26)	-0.51(11)	0.63(2)	-1.54(28)
^{156}Eu	17.51(66)	-1.34(15)	16.97(64)	-1.32(15)	0.63(3)	-2.44(25)
^{153}Gd	19.29(38)	-0.87(8)	17.59(34)	-0.82(8)	0.58(3)	-1.94(21)
^{155}Gd	19.35(34)	-0.67(13)	17.94(31)	-0.62(13)	0.58(2)	-1.74(22)
^{156}Gd	18.45(21)	0.36(9)	17.43(20)	0.39(8)	0.60(2)	-0.61(17)
^{157}Gd	18.36(44)	-0.70(12)	17.61(42)	-0.68(12)	0.59(2)	-1.63(20)
^{158}Gd	17.91(13)	0.28(8)	17.45(13)	0.29(8)	0.61(1)	-0.69(16)
^{159}Gd	17.71(27)	-0.71(12)	17.45(27)	-0.70(11)	0.61(2)	-1.68(19)
^{161}Gd	17.29(32)	-0.57(12)	17.53(32)	-0.57(12)	0.59(2)	-1.25(21)
^{160}Tb	18.20(24)	-1.28(11)	17.82(23)	-1.26(11)	0.61(2)	-2.39(20)
^{157}Dy	19.46(63)	-0.94(13)	18.06(58)	-0.90(13)	0.58(2)	-2.02(24)
^{159}Dy	17.62(91)	-0.86(17)	16.71(86)	-0.83(17)	0.62(4)	-1.75(29)
^{161}Dy	18.06(37)	-0.88(14)	17.51(36)	-0.86(14)	0.61(3)	-1.87(31)
^{162}Dy	18.08(21)	0.30(9)	17.81(20)	0.31(9)	0.60(1)	-0.58(15)
^{163}Dy	17.31(27)	-0.84(13)	17.36(27)	-0.84(13)	0.62(2)	-1.76(21)
^{164}Dy	17.75(23)	0.38(10)	18.06(24)	0.37(10)	0.60(1)	-0.42(15)
^{165}Dy	16.90(29)	-0.94(14)	17.32(30)	-0.96(14)	0.62(2)	-1.77(23)
^{166}Ho	18.29(27)	-1.00(9)	18.63(28)	-1.01(9)	0.59(1)	-1.94(16)
^{163}Er	19.20(50)	-0.80(12)	18.27(47)	-0.77(12)	0.58(2)	-1.78(21)
^{165}Er	18.34(40)	-0.74(10)	17.89(39)	-0.73(9)	0.60(2)	-1.72(17)
^{167}Er	18.19(24)	-0.65(10)	18.38(24)	-0.65(10)	0.60(1)	-1.50(17)
^{168}Er	17.79(15)	0.26(7)	18.17(16)	0.25(7)	0.60(1)	-0.62(14)
^{169}Er	17.57(25)	-0.67(11)	18.13(26)	-0.69(11)	0.60(2)	-1.43(24)
^{171}Er	17.67(41)	-0.68(16)	18.55(44)	-0.70(16)	0.59(2)	-1.33(26)
^{170}Tm	18.38(25)	-1.05(11)	18.79(26)	-1.07(11)	0.61(2)	-2.05(20)
^{171}Tm	19.39(49)	0.05(13)	19.83(54)	-0.02(14)	0.58(2)	-0.89(21)
^{169}Yb	19.90(65)	-0.50(10)	19.57(64)	-0.49(10)	0.55(3)	-1.33(23)
^{170}Yb	18.16(19)	0.38(11)	18.06(19)	0.38(11)	0.61(1)	-0.61(17)

TABLE II. (*Continued.*)

Nucleus	BSFG		BSFG with ED		CT	
	$a(\delta a)$ (MeV $^{-1}$)	$E_1(\delta E_1)$ (MeV)	$\tilde{a}(\delta \tilde{a})$ (MeV $^{-1}$)	$E_2(\delta E_2)$ (MeV)	$T(\delta T)$ (MeV)	$E_0(\delta E_0)$ (MeV)
^{171}Yb	18.47(37)	-0.45(9)	18.63(38)	-0.45(9)	0.58(2)	-1.21(17)
^{172}Yb	18.88(18)	0.32(8)	19.29(18)	0.31(8)	0.59(2)	-0.50(16)
^{173}Yb	18.34(38)	-0.25(18)	19.07(40)	-0.27(18)	0.57(2)	-0.89(30)
^{174}Yb	18.29(35)	0.45(17)	19.11(37)	0.43(17)	0.57(2)	-0.17(26)
^{175}Yb	17.91(35)	-0.41(13)	18.88(37)	-0.43(13)	0.58(2)	-1.06(21)
^{177}Yb	18.06(35)	-0.52(13)	19.18(38)	-0.54(13)	0.57(2)	-1.16(21)
^{176}Lu	19.55(30)	-0.71(8)	20.20(32)	-0.73(8)	0.56(1)	-1.57(13)
^{177}Lu	18.22(61)	-0.42(15)	18.74(64)	-0.43(15)	0.55(2)	-0.94(21)
^{175}Hf	19.08(55)	-0.53(10)	19.06(55)	-0.53(10)	0.57(2)	-1.28(19)
^{177}Hf	19.21(50)	-0.50(12)	19.55(52)	-0.51(12)	0.56(2)	-1.23(21)
^{178}Hf	19.07(24)	0.23(8)	19.57(25)	0.21(8)	0.57(2)	-0.58(24)
^{179}Hf	19.18(25)	-0.35(9)	19.81(26)	-0.37(9)	0.56(2)	-1.13(18)
^{180}Hf	17.86(22)	-0.03(10)	18.67(23)	-0.04(10)	0.59(2)	-0.80(22)
^{181}Hf	19.68(43)	-0.21(11)	20.72(46)	-0.24(11)	0.53(2)	-0.85(18)
^{181}Ta	20.52(49)	-0.29(15)	21.31(51)	-0.30(15)	0.54(2)	-0.87(26)
^{182}Ta	19.06(23)	-0.96(9)	19.96(25)	-0.99(9)	0.57(1)	-1.87(16)
^{183}Ta	17.70(46)	-0.76(17)	18.44(49)	-0.79(17)	0.60(2)	-1.51(26)
^{181}W	19.07(75)	-0.55(15)	19.64(77)	-0.56(16)	0.58(3)	-1.38(26)
^{183}W	19.22(30)	-0.24(10)	20.24(33)	-0.27(11)	0.55(2)	-0.92(17)
^{184}W	18.76(30)	0.08(14)	19.72(33)	0.04(14)	0.58(2)	-0.64(21)
^{185}W	19.45(28)	-0.50(8)	20.54(30)	-0.52(8)	0.56(1)	-1.30(14)
^{187}W	19.14(36)	-0.81(13)	20.44(40)	-0.85(14)	0.57(2)	-1.63(22)
^{186}Re	19.87(28)	-0.90(10)	21.05(31)	-0.93(10)	0.56(1)	-1.76(18)
^{188}Re	19.93(26)	-1.00(10)	21.45(29)	-1.04(10)	0.55(1)	-1.88(17)
^{187}Os	19.07(29)	-0.78(11)	20.08(32)	-0.81(11)	0.58(2)	-1.57(19)
^{188}Os	19.88(37)	0.34(12)	21.23(37)	0.32(11)	0.58(2)	-0.63(19)
^{189}Os	18.60(38)	-1.04(15)	19.97(42)	-1.08(15)	0.59(2)	-1.87(25)
^{190}Os	19.44(26)	0.29(11)	21.32(29)	0.24(12)	0.56(2)	-0.33(20)
^{191}Os	18.29(37)	-1.07(13)	20.39(43)	-1.14(13)	0.60(2)	-1.91(21)
^{193}Os	18.06(42)	-1.00(19)	21.24(54)	-1.11(20)	0.59(3)	-1.69(30)
^{192}Ir	19.45(45)	-1.55(13)	21.77(53)	-1.65(13)	0.60(2)	-2.74(22)
^{193}Ir	22.77(58)	-0.30(9)	26.11(67)	-0.38(9)	0.52(2)	-1.21(15)
^{194}Ir	17.98(61)	-1.66(15)	21.23(75)	-1.84(17)	0.64(3)	-2.78(25)
^{195}Pt	19.15(78)	-1.02(17)	21.55(90)	-1.10(18)	0.58(3)	-1.87(27)
^{195}Pt	15.30(79)	-1.57(24)	18.25(99)	-1.77(26)	0.72(5)	-2.43(36)
^{196}Pt	17.97(29)	0.38(10)	22.53(38)	0.21(10)	0.61(2)	-0.33(18)
^{197}Pt	14.91(63)	-1.61(25)	18.99(89)	-1.90(29)	0.72(4)	-2.38(39)
^{199}Pt	16.06(64)	-1.25(23)	22.16(101)	-1.57(27)	0.66(4)	-1.90(35)
^{198}Au	16.00(22)	-1.72(16)	20.98(36)	-2.12(18)	0.71(3)	-2.74(35)
^{199}Hg	15.82(69)	-1.27(26)	21.56(107)	-1.66(31)	0.69(4)	-2.02(40)
^{200}Hg	14.29(26)	-0.62(19)	19.79(45)	-1.22(23)	0.77(4)	-1.40(37)
^{201}Hg	13.39(54)	-1.78(31)	19.45(98)	-2.46(40)	0.80(5)	-2.46(46)
^{202}Hg	13.79(56)	-0.61(22)	20.93(102)	-1.38(29)	0.77(4)	-1.23(31)
^{204}Tl	12.90(41)	-1.96(28)	20.45(94)	-3.21(40)	0.84(4)	-2.72(42)
^{206}Tl	10.41(54)	-1.25(32)	18.33(136)	-3.13(53)	0.98(7)	-1.62(44)
^{205}Pb	12.71(56)	-0.61(22)	21.47(114)	-1.60(31)	0.81(4)	-1.08(30)
^{207}Pb	11.08(54)	0.60(42)	19.85(158)	-1.73(67)	0.91(9)	0.23(57)
^{208}Pb	10.01(60)	1.17(39)	18.41(168)	-0.67(64)	1.06(11)	0.52(67)
^{209}Pb	11.22(58)	0.61(55)	27.12(355)	0.31(51)	0.77(12)	0.69(49)
^{210}Bi	11.40(49)	-1.24(29)	19.73(118)	-2.21(42)	0.82(8)	-1.43(53)
^{227}Ra	24.33(65)	-0.86(12)	22.91(60)	-0.84(12)	0.46(2)	-1.56(20)
^{229}Th	25.35(88)	-0.77(15)	24.01(179)	-0.76(15)	0.45(3)	-1.49(22)
^{230}Th	24.33(46)	0.05(9)	23.13(43)	0.06(8)	0.47(1)	-0.59(14)
^{231}Th	26.41(41)	-0.42(8)	25.17(39)	-0.40(7)	0.43(2)	-1.16(17)
^{233}Th	25.98(34)	-0.58(9)	24.75(32)	-0.57(9)	0.43(1)	-1.29(15)
^{233}Pa	22.27(44)	-0.98(9)	21.32(42)	-0.96(9)	0.53(2)	-1.87(16)

TABLE II. (*Continued.*)

Nucleus	BSFG		BSFG with ED		CT	
	$a(\delta a)$ (MeV $^{-1}$)	$E_1(\delta E_1)$ (MeV)	$\tilde{a}(\delta \tilde{a})$ (MeV $^{-1}$)	$E_2(\delta E_2)$ (MeV)	$T(\delta T)$ (MeV)	$E_0(\delta E_0)$ (MeV)
^{234}Pa	28.01(62)	-0.70(13)	26.92(59)	-0.69(13)	0.41(2)	-1.37(23)
^{233}U	25.37(43)	-0.51(9)	24.69(42)	-0.50(9)	0.45(1)	-1.17(16)
^{234}U	25.24(22)	0.30(6)	24.52(21)	0.30(6)	0.45(1)	-0.38(11)
^{235}U	25.08(30)	-0.51(9)	24.44(29)	-0.50(9)	0.45(2)	-1.22(20)
^{236}U	25.76(21)	0.14(7)	25.07(20)	0.15(7)	0.44(1)	-0.46(13)
^{237}U	25.60(39)	-0.43(12)	25.04(38)	-0.42(12)	0.43(2)	-1.02(23)
^{238}U	25.26(35)	0.06(8)	24.48(34)	0.07(8)	0.45(1)	-0.59(14)
^{239}U	26.67(31)	-0.31(9)	25.95(30)	-0.30(9)	0.42(2)	-0.92(18)
^{237}Np	25.01(27)	-0.40(6)	24.47(26)	-0.39(6)	0.47(1)	-1.14(12)
^{238}Np	25.96(33)	-0.84(11)	25.55(32)	-0.84(11)	0.45(2)	-1.64(24)
^{239}Np	25.26(58)	-0.63(8)	24.65(55)	-0.62(8)	0.46(1)	-1.34(15)
^{239}Pu	25.23(49)	-0.30(11)	25.22(49)	-0.30(11)	0.45(1)	-0.91(14)
^{240}Pu	25.16(20)	0.12(8)	24.97(20)	0.13(8)	0.46(1)	-0.50(15)
^{241}Pu	26.03(29)	-0.32(7)	25.86(29)	-0.32(7)	0.42(1)	-0.90(13)
^{242}Pu	28.97(51)	0.34(10)	28.57(50)	0.34(10)	0.40(1)	-0.22(15)
^{243}Pu	27.20(40)	-0.19(7)	26.93(39)	-0.19(7)	0.41(1)	-0.74(12)
^{245}Pu	27.63(64)	-0.19(12)	27.20(62)	-0.19(12)	0.39(2)	-0.57(20)
^{242}Am	26.19(23)	-0.74(7)	26.22(23)	-0.74(7)	0.44(1)	-1.49(15)
^{243}Am	26.42(48)	-0.43(8)	26.20(47)	-0.43(8)	0.44(1)	-1.05(15)
^{244}Am	26.02(29)	-0.84(7)	25.96(29)	-0.84(7)	0.45(1)	-1.67(12)
^{243}Cm	24.39(43)	-0.26(9)	24.70(44)	-0.26(9)	0.46(1)	-0.82(15)
^{244}Cm	24.63(61)	0.17(16)	24.92(62)	0.17(16)	0.46(2)	-0.34(23)
^{245}Cm	24.96(33)	-0.39(8)	25.38(34)	-0.40(8)	0.45(1)	-0.99(13)
^{246}Cm	27.56(44)	0.42(7)	27.81(45)	0.42(7)	0.42(1)	-0.29(12)
^{247}Cm	23.64(54)	-0.62(12)	23.89(54)	-0.62(12)	0.47(2)	-1.17(20)
^{248}Cm	25.03(62)	0.29(13)	24.99(62)	0.30(13)	0.43(2)	-0.18(25)
^{249}Cm	25.53(57)	-0.57(10)	25.42(57)	-0.56(10)	0.43(2)	-1.11(16)
^{250}Bk	25.86(38)	-0.94(9)	25.95(38)	-0.95(9)	0.44(1)	-1.66(16)
^{250}Cf	24.74(35)	0.20(9)	25.42(36)	0.19(9)	0.45(1)	-0.31(16)
^{251}Cf	26.34(49)	-0.43(7)	26.96(50)	-0.43(7)	0.42(1)	-0.99(13)

T , which has an average dependence on mass as $A^{-2/3}$ [11], can be also well correlated with the shell correction. The dependence on $A^{-2/3}$ shows that the temperature T decreases with increasing surface of the nucleus, because the surface nucleons are first excited. Bohr and Mottelson [16] define the temperature as $T \sim E/n_{\text{ex}}$, the average energy per excited nucleon, and n_{ex} seems to be proportional to the surface. The parameter \tilde{a} has an almost linear behavior with mass, as proposed in Ref. [7].

We used the definition of the shell correction S given by Eq. (7). For the macroscopic liquid drop-mass calculation, we chose the recent Weizsäcker type formula proposed by Pearson [17], which gives a good description of nearly 2000 nuclear masses with just five parameters. This formula does not contain shell and pairing effects. With the definition of the nuclear binding energy as $E_b = NM_n + ZM_p - M(N, Z)c^2$, and $M(N, Z)$ the nuclear mass, this formula reads [17]

$$-\frac{E_b}{A} = a_{\text{vol}} + a_{\text{sf}} A^{-1/3} + \frac{3e^2}{5r_0} Z^2 A^{-4/3} + (a_{\text{sym}} + a_{\text{ss}} A^{-1/3}) \left(\frac{N-Z}{A} \right)^2, \quad (9)$$

with the parameter values (fitted to about 2000 mass values) being $a_{\text{vol}} = -15.65$ MeV, $a_{\text{sf}} = 17.63$ MeV, $a_{\text{sym}} = 27.72$ MeV, $a_{\text{ss}} = -25.60$ MeV, and $r_0 = 1.233$ fm. The shell correction $S(Z, N)$ [Eq. (7)], calculated from experimental masses [18] and this mass formula, is given in Table I and also shown in the first panel of Fig. 4. As previously commented, the LD parameters a and T (Fig. 1) are very well correlated with this quantity.

The S values in Fig. 4 show slightly different curves for even-even, odd, and odd-odd nuclei. Consequently a pairing correction has to be applied:

$$S' = S - \Delta. \quad (10)$$

Various types of pairing corrections Δ were introduced in the fit procedures of a and T . The best results were obtained with

$$\Delta = \begin{cases} +0.5P_d, & \text{for even-even} \\ 0, & \text{for odd-A} \\ -0.5P_d, & \text{for odd-odd nuclei.} \end{cases} \quad (11)$$

The fitted factor in front of P_d was always within the error bars close to 0.5 or 0.0; therefore we set it fixed to 0.5 or 0.0, respectively, because this is also reasonable from the physics

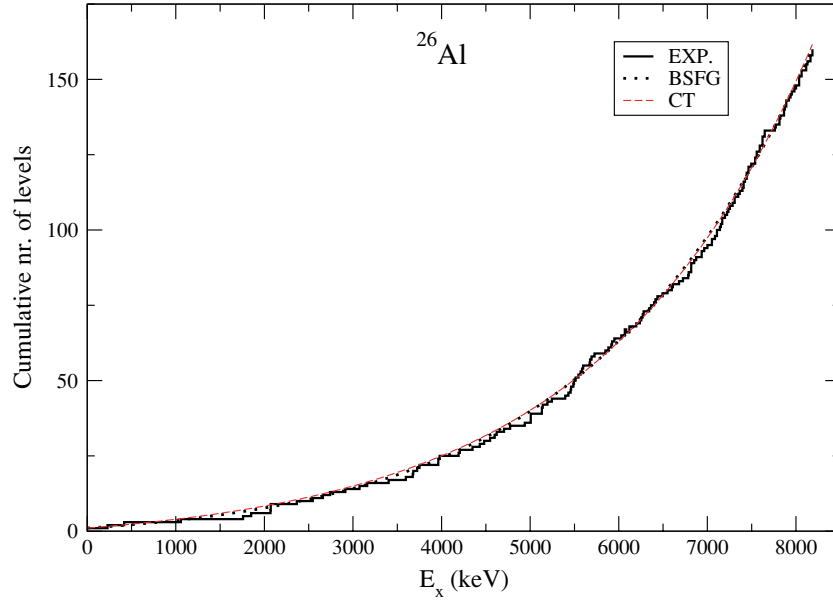


FIG. 1. (Color online) Fits of the experimental cumulative number of levels of ^{26}Al with spin $0-5\hbar$ with the BSFG and CT model formulas.

point of view. P_d is the so-called deuteron pairing [18,19] calculated from mass tables in a similar way as P_n and P_p :

$$P_d = \frac{1}{4}(-1)^{Z+1}[S_d(A+2, Z+1) - 2S_d(A, Z) + S_d(A-2, Z-1)],$$

where S_d is the deuteron separation energy. The P_d values are shown in Fig. 4. They are very similar for even-even and odd-odd nuclei and smaller, close to 0.0, for odd-mass nuclei.

D. Correlations of E_1 , E_2 , and E_0

Inspection of Fig. 2 demonstrates that the backshift curves are quite different for even-even, odd, and odd-odd nuclei. The curves for the even-even nuclei are relatively smooth, whereas the odd-odd nuclei exhibit more fluctuations and odd nuclei have strong variations. Therefore a pairing correction has to be introduced. Again, comparison of various pairing corrections showed that P_d is the best choice. Indeed, by comparing Figs. 2 and 4, one can realize that some fraction of P_d describes already rather well the behavior of E_1 , E_2 , and E_0 .

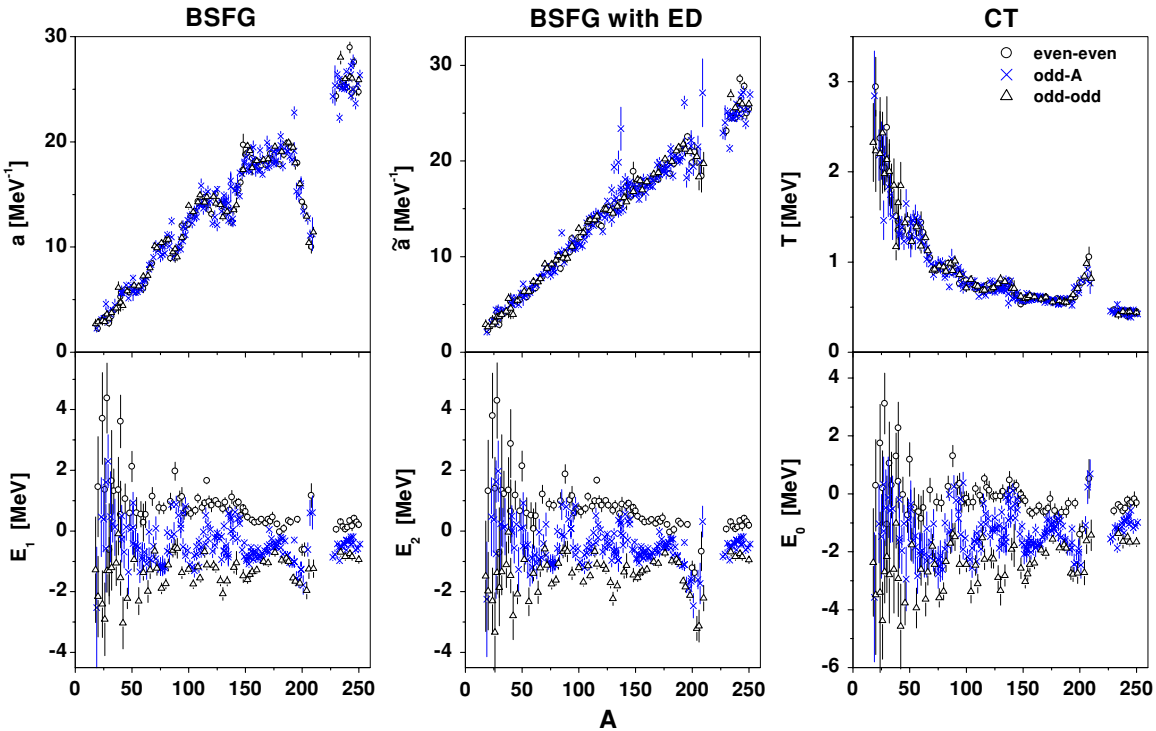
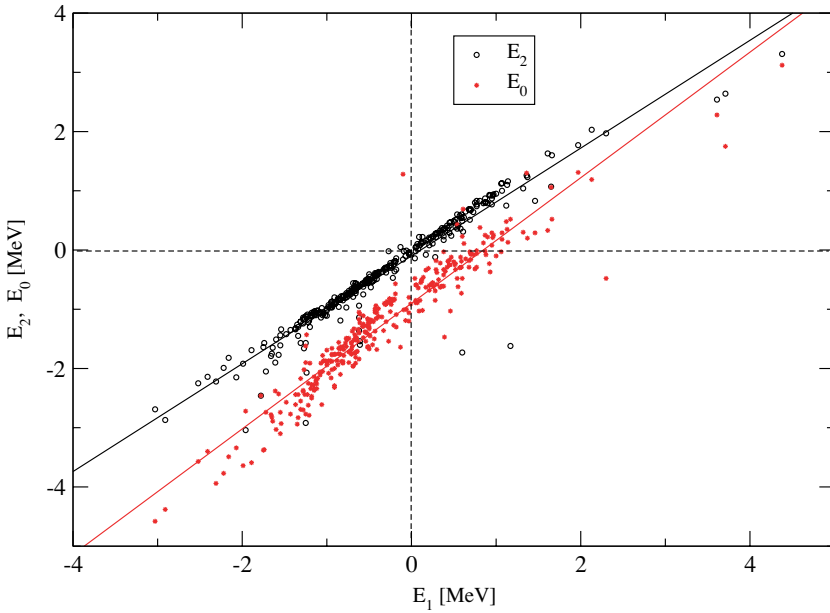


FIG. 2. (Color online) Phenomenological LD parameters for the three models considered in this work (see text for details).



In particular, P_d appears to be a natural choice for the backshifts of the odd- A nuclei, as it has smaller values than those for

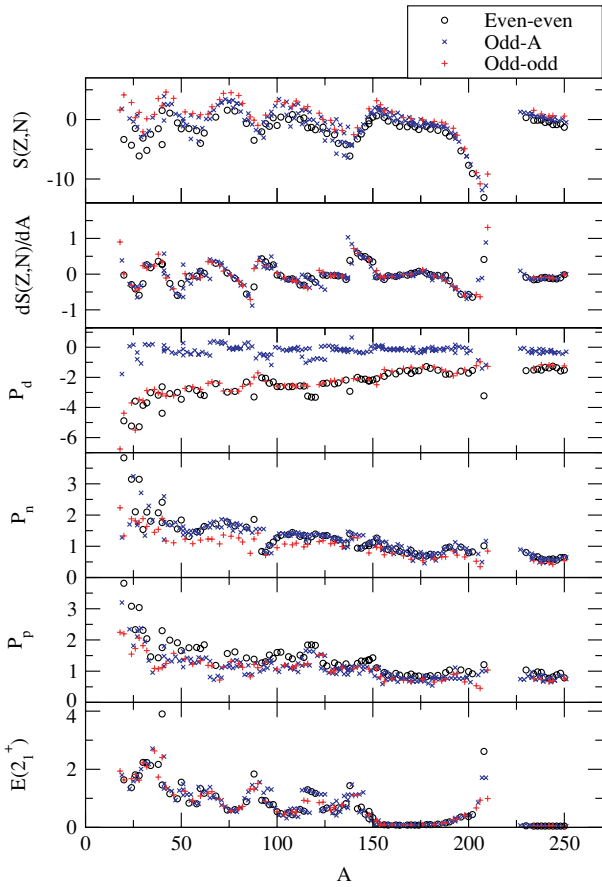


FIG. 4. (Color online) Different physical quantities used to find correlations with the LD phenomenological parameters (all in mega-electron-volts). S is the shell correction [Eqs. (7) and (9)], dS/dA is its derivative [Eq. (12)], P_d is the deuteron pairing energy. See text for more details.

FIG. 3. (Color online) The linear correlations between the backshift energies of the three models. The straight line fitted to the E_2 versus E_1 correlation passes through the origin and has a slope close to 1.

the even-even and odd-odd nuclei, and, moreover, it has a behavior that correlates well with some of the variations observed in these backshifts. A closer look at these correlations showed that some structures in the backshifts E_i remain still unaccounted for—for example, the oscillation around mass 200, which is due to the 82 shell closure. This structure, as well as some other, smaller details, were found to be well correlated with the derivative of the shell correction $S(Z, N)$ of Eq. (7) with respect to A . We calculate this numerically from the mass tables; it can be calculated in many ways, from differences of masses of two nearby nuclei, but, because we found that deuteron mass differences have some relevance for our problem, we calculate this as

$$\frac{dS(Z, N)}{dA} = [S(Z + 1, N + 1) - S(Z - 1, N - 1)]/4. \quad (12)$$

This derivative is also given in the seventh column of Table I, and is shown in Fig. 4.

Other quantities that we have considered when looking for useful correlations were (i) the energy of the first excited (2_1^+) state in the even-even nuclei (and averages of this value on the neighboring nuclei in the case of the odd- A and odd-odd nuclei). This quantity is also shown in Fig. 4. As is well known, its variations reflect the effects of the shell closures and collectivity. (ii) Alternatively, we considered the quadrupole deformation parameter ε_2 as calculated by Möller and Nix [20]. One could find some good correlations between these quantities and the structures in our parameters, but not better than those with the other quantities in Fig. 4. In addition, when nuclei far from stability were considered, relying on such quantities as $E(2_1^+)$ and/or ε_2 would have required the use of other extrapolation methods or of some model.

E. Fit with simple formulas

Finally, our procedure was to fit the LD parameters of Fig. 2 with simple formulas, in general linear (or at most

quadratic) combinations of quantities from Fig. 4 with which we recognize useful correlations: $S(Z, N)$, $dS(Z, N)/dA$, P_d , and the mass number A . As already mentioned, we have studied a large number of such formulas with up to ten parameters and have selected those with a good χ^2 . Because these formulas were empirical, we have finally preferred those with less parameters, and with some symmetry. As was emphasized, for a and T , the deuteron pairing P_d was initially multiplied with an arbitrary coefficient, but after the data were fit, this was found to converge toward values close to either 1.0 or 0.5, which were subsequently kept in the final fit.

1. The BSFG model

There is a very clear correlation between the a parameter and the shell correction $S(Z, N)$, which has been observed since the work of Ref. [3]. As already explained, we observed that the fit of a/A is improved if we use S' of Eq. (10) instead of S and we add a small A dependence. Therefore the formula adopted for a/A is

$$a/A = p_1 + p_2 S'(Z, N) + p_3 A \quad \text{for all nuclei}, \quad (13)$$

with the p_1 , p_2 , and p_3 constants given in Table III.

For the backshift energy parameter E_1 the adopted formula is

$$E_1 = \begin{cases} p_1 - 0.5P_d + p_4 \frac{dS(Z, N)}{dA}, & \text{even-even} \\ p_2 - 0.5P_d + p_4 \frac{dS(Z, N)}{dA}, & \text{odd-A} \\ p_3 + 0.5P_d + p_4 \frac{dS(Z, N)}{dA}, & \text{odd-odd}, \end{cases} \quad (14)$$

TABLE III. Summary of formulas (13)–(18) proposed for the description of the phenomenological model parameters (Fig. 2). The quantities P_d , $S(Z, N)$, and $dS(Z, N)/dA$ are given in MeV (Table I); therefore the dimensions of the different p_i constants in the formulas are such that a , \tilde{a} are in MeV^{-1} , and T , E_i are in MeV, respectively. Also note that for the compactness of the table we use the same notation, p_i , for the fitted parameters in the different formulas; however, for example in the case of the BSFG, the p_i constants in the formula of a and of E_1 have different meanings (they are factors for different quantities and have completely different values).

Model	Formula	Parameters in the formula				Type of nuclei
		p_1	p_2	p_3	p_4	
BSFG	$a/A = p_1 + p_2 S'(Z, N) + p_3 A$	0.127(1)	$4.98(13) \times 10^{-3}$	$-8.95(53) \times 10^{-5}$		All
	$E_1 = p_1 - 0.5P_d + p_4 \frac{dS(Z, N)}{dA}$	-0.468(30)	-0.565(23)	-0.231(39)	0.438(83)	e-e
	$= p_2 - 0.5P_d + p_4 \frac{dS(Z, N)}{dA}$					o-e,e-o
	$= p_3 + 0.5P_d + p_4 \frac{dS(Z, N)}{dA}$					o-o
BSFG-ED	$\tilde{a}/A = p_1 + p_3 A$	0.127(1)		$-9.05(53) \times 10^{-5}$		All
	$E_2 = p_1 - 0.5P_d + p_4 \frac{dS(Z, N)}{dA}$	-0.477(31)	-0.577(23)	-0.231(40)	0.442(87)	e-e
	$= p_2 - 0.5P_d + p_4 \frac{dS(Z, N)}{dA}$					o-e,e-o
	$= p_3 + 0.5P_d + p_4 \frac{dS(Z, N)}{dA}$					o-o
CT	$TA^{2/3} = p_1 + p_2 S'(Z, N) + p_3 S'(Z, N)^2$	17.45(6)	-0.51(4)	0.051(10)		All
	$E_0 = p_1 - 0.5P_d + p_2 \frac{dS(Z, N)}{dA}$	-1.23(3)	0.32(14)	-1.42(3)	0.84(14)	e-e
	$= p_3 - P_d + p_4 \frac{dS(Z, N)}{dA}$					o-e,e-o
	$= p_1 + 0.5P_d + p_2 \frac{dS(Z, N)}{dA}$					o-o

Notes: $S(Z, N) = M_{\text{exp}} - M_{\text{LD}}$, see Eqs. (7) and (9); $S'(Z, N) = S(Z, N) - \Delta$, see Eqs. (10) and (11); $P_d = \frac{1}{4}(-1)^{Z+1}[S_d(A+2, Z+1) - 2S_d(A, Z) + S_d(A-2, Z-1)]$; (S_d is the deuteron separation energy) [18,19].

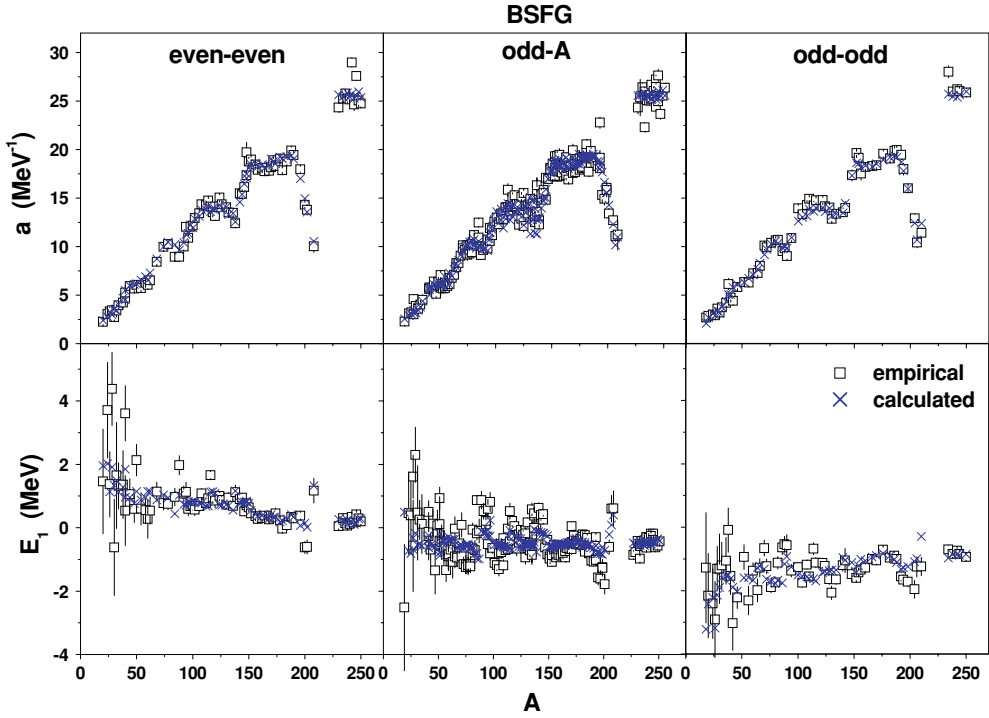


FIG. 5. (Color online) Fits to the BSFG model parameters (Fig. 1) with empirical formulas (13) and (14) and p_i values from Table III.

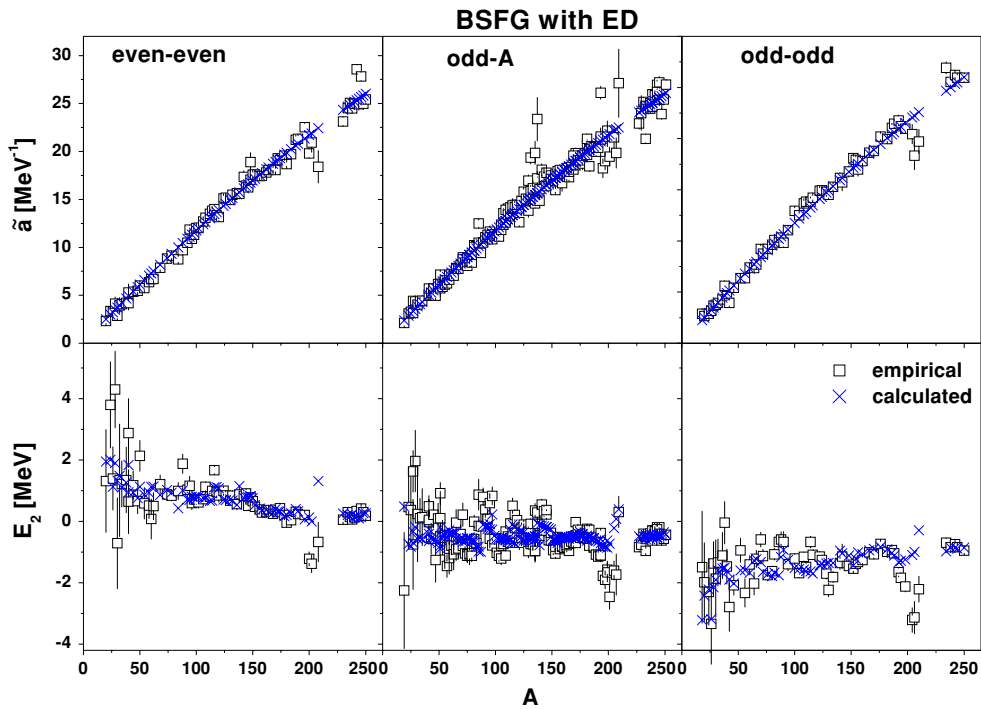


FIG. 6. (Color online) Same as Fig. 5, but for the BSFG-ED model, formulas (15) and (16). Note that the p_i parameters found from fit (Table III) are identical with those of the BSFG model.

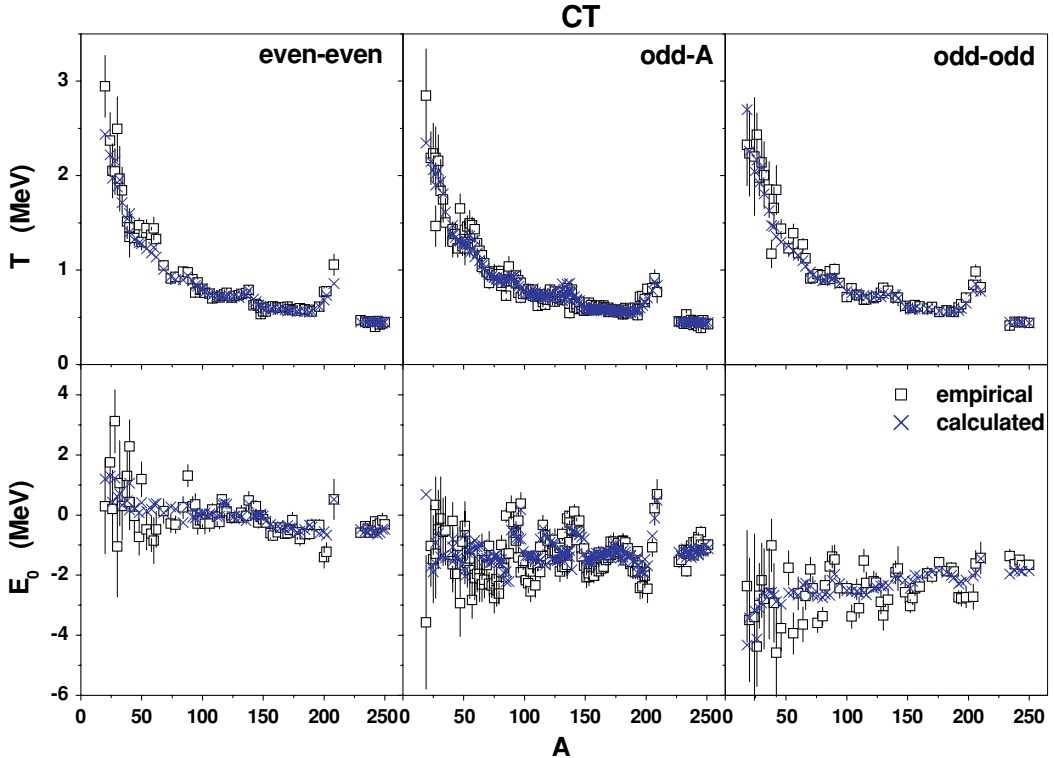


FIG. 7. (Color online) Same as Fig. 5 but for the CT model, formulas (17) and (18).

equivalent; the only difference between them is the way each of these models uses the shell correction term $S(Z, N)$.

3. The CT model

For the CT model the fitted formulas are

$$TA^{2/3} = p_1 + p_2 S' + p_3 S'^2 \quad (17)$$

and

$$E_0 = \begin{cases} p_1 - 0.5 P_d + p_2 \frac{dS(Z,N)}{dA}, & \text{even-even} \\ p_3 - P_d + p_4 \frac{dS(Z,N)}{dA}, & \text{odd-A} \\ p_1 + 0.5 P_d + p_2 \frac{dS(Z,N)}{dA}, & \text{odd-odd}, \end{cases} \quad (18)$$

which is similar to Eqs. (13) and (15). The values of the fitted parameters and the fits are shown in Table III and Fig. 7, respectively.

IV. CONCLUSIONS

Figure 8 shows a detailed comparison between the experimental neutron resonance density and the one calculated with the empirical formulas already presented (with the parameter values from Table III). It can be seen that for both the BSFG and BSFG-ED models the experimental data are reproduced within a factor of 2; for less than 10% of the data the agreement is worse. For the CT model the general agreement is somewhat weaker. In all three models

there are still problems near $N = 50$ and $N = 82$, whereas in other regions a smooth behavior and good agreement are observed.

The result of our investigation is a new set of nuclear LD parameters for 310 nuclei between ^{19}F and ^{251}Cf for three two-parameter models (BSFG, BSFG-ED, and CT), which we obtained by fitting the newest complete experimental data for both the low-energy excited states and the LD at the neutron binding energy. The empirical LD model parameters for all nuclei have been described by simple formulas with few parameters. Figures 5–7 show that the simple formulas proposed, Eqs. (13)–(18), with the parameters given in Table III, describe reasonably well the whole set of empirical LD parameters (Table II). It is remarkable that these formulas describe also the main features of the backshift energies E_i that were determined from the data as free fit parameters.

The proposed formulas involve only the “shell correction” (the difference between the experimental mass and the mass calculated with a macroscopic formula), its derivative with respect to the mass, and the deuteron pairing energy P_d . All these quantities can be taken or derived from the mass tables [18], so in essence our formulas calculate the LDs from nuclear masses. The formulas do not depend on any model; in extrapolating them to nuclei far from stability we only have to rely on the methods of extrapolation developed for the nuclear masses [21]. This means also that the coarse structure of the nuclei at higher excitations is mainly determined by the mass of the ground state. It should be emphasized that our results show

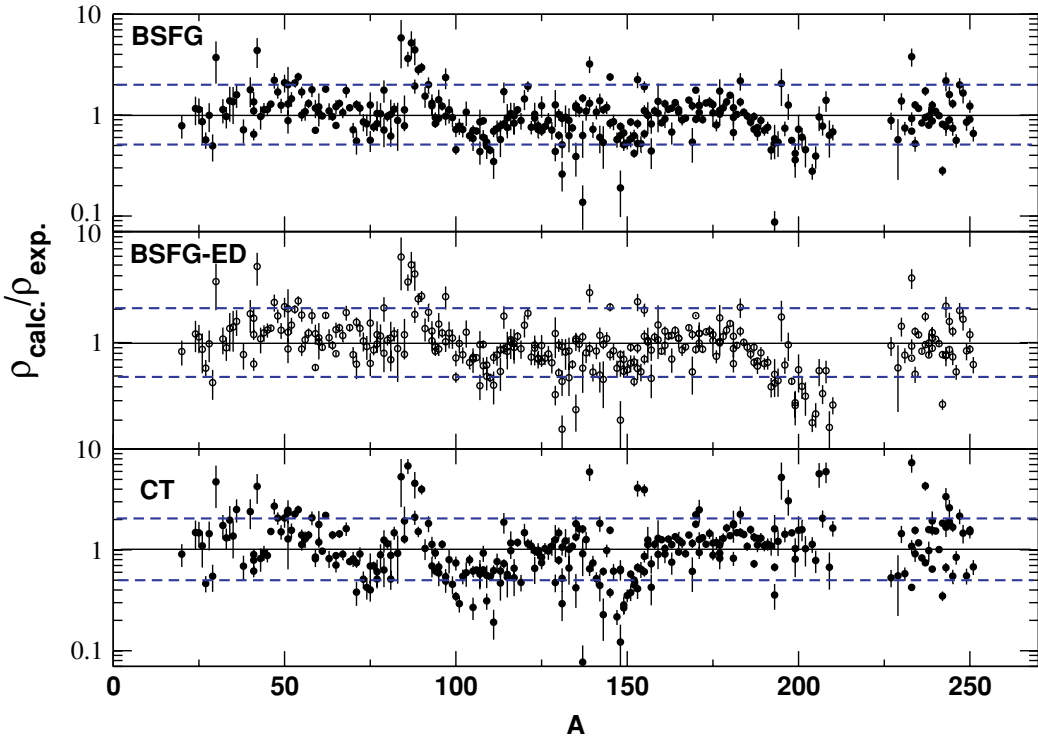


FIG. 8. (Color online) Test of the formulas proposed in this work for the LD at the neutron resonance energy. The dashed lines mark a difference by a factor of 2 between the experimental and the calculated values.

that special enhancement factors, e.g., for rotational nuclei, are not required.

Our formulas (13)–(18) (with parameter values from Table III) are completely empirical. Their derivation is based on the observation of the correlations between the phenomenological LD parameters and the (mass related) quantities entering these formulas. It remains a challenge for the theory to justify such empirical formulas. Because we did not guide ourselves on theoretical approaches to the LDs, it may be that we have not chosen the “most appropriate” functional forms. Nevertheless, this empirical study highlights a few points that need a deeper understanding. First, the finding that the deuteron pairing energy is more useful for the description of the LD parameters than the neutron and proton pairings (or their smooth description $\delta = 12/\sqrt{A}$), which were the only ones considered until now, is remarkable. Then, the finding that the inclusion of the derivative of the shell correction with respect to the mass helps to describe better the LDs is equally interesting.

The present method of calculating LD parameters for nuclei for which there are no experimental data available, not from some local systematics and/or by some arbitrary extrapolation, but by use of the formulas proposed in this paper, seems to be a reasonable means of extrapolation to nuclei far from stability. The BSFG and CT models with parameters calculated with formulas (13) and (14) and (17) and (18), respectively, may be safely used up to the neutron binding energy or slightly higher energies. The BSFG-ED model (BSFG with an energy-dependent LD parameter), formulas (15) and (16), may be recommended up to higher energies (~ 15 – 20 MeV), because it contains the recommended damping of the shell effects with increasing excitation energy.

ACKNOWLEDGMENTS

We thank G. Audi, T. Belgya, R. Capote Noy, R. F. Casten, M. Herman, and F.-K. Thielemann for fruitful discussions and for providing data.

-
- [1] A. V. Ignatyuk, Rep. IAEA-TECDOC-1034 (International Atomic Energy Agency, Vienna, 1998), p. 65.
 - [2] P. Demetriou and S. Goriely, Nucl. Phys. **A695**, 95 (2001).
 - [3] A. Gilbert and A. G. W. Cameron, Can. J. Phys. **43**, 1446 (1965); P. J. Brancazio and A. G. W. Cameron, *ibid.* **47**, 1029 (1969).
 - [4] W. Dilg, W. Schantl, H. Vonach, and M. Uhl, Nucl. Phys. **217**, 269 (1973).
 - [5] D. Bucurescu and T. von Egidy, presented at the NUSTAR’05 Conference (Guidford, U.K., 5–8 Jan., 2005) J. Phys. G: Nucl. Part. Phys. **31**, S1675 (2005).
 - [6] H. Zhongfu, H. Ping, S. Zongdi, and Z. Chunmei, Chin. J. Nucl. Phys. **13**, 147 (1991).

- [7] A. V. Ignatyuk, G. N. Smirenkin, and A. S. Tishin, Sov. J. Nucl. Phys. **21**, 255 (1975).
- [8] A. V. Ignatyuk, K. K. Istekov, and G. N. Smirenkin, Sov. J. Nucl. Phys. **29**, 450 (1979).
- [9] T. Rauscher, F.-K. Thielemann, and K.-L. Kratz, Phys. Rev. C **56**, 1613 (1997).
- [10] A. S. Iljinov, M. V. Mebel, N. Bianchi, E. De Sanctis, C. Guaraldo, V. Lucherini, V. Muccifora, E. Polli, A. R. Reolon, and P. Rossi, Nucl. Phys. **A543**, 450 (1979).
- [11] T. von Egidy, H. H. Schmidt, and A. N. Behkami, Nucl. Phys. **A481**, 189 (1988).
- [12] R. B. Firestone *et al.*, *Table of Isotopes* (Wiley, New York, 1996), and the ENSDF database.
- [13] G. Reffo, Rep. IAEA-TECDOC-1034 (International Atomic Energy Agency, Vienna, 1998), p. 25; R. Capote Noy, personal communication (2004) and the RIPL-2 database: <http://www-nds.iaea.org>
- [14] Po-lin Huang, S. M. Grimes, and T. N. Massey, Phys. Rev. C **62**, 024002 (2000).
- [15] S. I. Al-Quraishi, S. M. Grimes, T. N. Massey, and D. A. Resler, Phys. Rev. C **63**, 065803 (2001); **67**, 015803 (2003).
- [16] A. Bohr and B. R. Mottelson, *Nuclear Structure* (Benjamin, New York/Amsterdam, 1969), Vol. I, p. 155.
- [17] J. M. Pearson, Hyperfine Interact. **132**, 59 (2001).
- [18] G. Audi, A. H. Wapstra, and C. Thibault, Nucl. Phys. **A729**, 337 (2003).
- [19] The AME2003 files, retrieved from <http://csnwww.in2p3.fr/amdc>
- [20] P. Möller and J. R. Nix, At. Data Nucl. Data Tables **59**, 95 (1995).
- [21] A. H. Wapstra, G. Audi, and C. Thibault, Nucl. Phys. **A729**, 129 (2003).